Tailoring Aggregation of Thiophene-based Polymers Using Solvent and Solvent Additives

By
Werkitu Geremew Dabale

A Thesis Submitted to the
Department of Physics of Addis Ababa University
As Part of the Requirements for the Degree of
Master of Science in Physics (Polymer Physics)

Supervisor:

Dr. Newayemedhin Aberra (Assoc. Prof.)

November 15, 2024

ADDIS ABABA UNIVERSITY

DEPARTMENT OF PHYSICS

The undersigned hereby certify that they have read and recommend to the College of Natural and Computational Sciences for acceptance a thesis entitled

" **Tailoring Aggregation of Thiophene-based Polymers Using Solvent and Solvent Additives**" by

Werkitu Geremew Dabale

in partial fulfillment of the requirements for the degree of

Master of Science in Physics.

Date: _____

Approved by the Examination Committee (Name and Signature)

External Examiner: _____

Internal Examiner: _____

Advisor: Dr. Newayemedhin Abera (Associate Professor)_____

Chairman: _____

I, **Werkitu Geremew Dabale**, hereby declare that the work presented in this thesis titled **"Tailoring Aggregation of Thiophene-based Polymers Using Solvent and Solvent Additives"** is my own original work, except where due acknowledgment has been made. To the best of my knowledge and belief, this thesis contains no material previously published or written by another person, nor material that has been accepted for the award of any other degree or diploma at any university or other institution of higher learning.

Any contributions or sources from the work of others, whether published or unpublished, have been duly cited and acknowledged in accordance with academic standards.

Signature: _____

Date: _____

ADDIS ABABA UNIVERSITY

Date: Nov.6 2024

Author: Werkitu Geremew Dabale

Title: Tailoring Aggregation of Thiophene-based Polymers Using Solvent and Solvent Additives

Department: Physics

Degree: MSc

Convocation:

_____

Signature of Author

DEDICATION

To my husband Tamiru Tadasse,

my baby boy Firaol Tamiru and to all my family members.

ACKNOWLEDGEMENT

First of all, thanks to God, the almighty power for give me the authority to complete this MSc thesis study in spite of the ups and down of the life. Then, I would like to express my deepest thankfulness, sincere and profound gratitude to my supervisor, Dr. Newayemedhin Abera (Associate Professor) for her encouragement, guidance, patience, continual support and constructive comments throughout the development of this study. She has strong academic skills and passion for a model of scientific research and generous mentorship. I appreciate her incommensurable knowledge, skill, attitude and genuineness for science. I am happy to thanks minister of education (MOE) for hosting me for sponsoring and joining to Addis Ababa University (AAU) to peruse my MSc study. I would like to thanks all the members of Physics departments in AAU for their efforts to finalize this Msc study. I would also like to acknowledge all the material physics and polymer physics research group members in the department of physics in AAU, especially Alemayehu Girma and Gizaw Birhanu for their unreserved time, energy and knowledge for helping the development of the study. My deepest thanks also goes to my husband Tamiru Tadasse, my friends Admasu Kumsa, and my brother Kebede Geremew who have made my life inside and outside of home a lot more interesting for engaging their work. They have been give advice for a constant source of encouragement and wonderful time. Finally, I would like to say thank you to my husband Tamiru Tadasse for tolerating and helping me for pursuit my dreams. I wish, God blessed you.

Contents

List of Figures

List of Tables

Abbreviation

OLED	organic light emitting diodes
OPV	organic photovoltaics
CF	chloroform
oDCB	1,2-dichlorobenzene
OSC	organic solar cell
PCE	power conversion efficiency
D	donor
A	acceptor
D-A	donor-acceptor
FET	field effect transistor
P3HT	poly 3-hexylthiophene
P1TI	poly 1-thiophene isoindigo
PPV	poly phenylene vinylene
F8BT	poly 8-dioctylfluorene alt-benzothiadiazole
PV	photovoltaic
JC	Coulomb Coupling
H_2O	water
PL	Photoluminescence
E_g	Band gap energy

Abstract

With an emphasis on P3HT and P1TI, this thesis examines how H and J aggregation affects the photophysical characteristics and charge production mechanisms in donor-acceptor (D-A) copolymers. Because of their promising charge transport and exciton mobility properties, these polymers are especially interesting for organic optoelectronic devices, such as organic photovoltaics (OPVs) and organic light-emitting diodes (OLEDs). But there is still a lack of thorough knowledge on how aggregation behavior affects their optical and electrical characteristics, especially when it comes to the effects of solvent conditions and high boiling point additives on the aggregation mechanisms of H and J. The copolymers were produced and deposited as thin films on cleaned glass substrates using thiophene-based derivatives as donor components and isoindigo as acceptor. Several solvents, including 1,2-dichlorobenzene (o-DCB), were used to create the films. chloroform (CF), selected according to their polarity and refractive indices.Higher A00/A01 and I00/I01 ratios in both P3HT and P1TI demonstrated that o-DCB promoted J-aggregation, according to experimental results. This led to better chain ordering and exciton delocalization, both of which are advantageous for charge transfer in OPVs. On the other hand, CF encouraged H-aggregation, which resulted in less exciton mobility and more localized exciton states. It was discovered that adding the high boiling point additive DIO improved charge separation, decreased H-aggregation, and increased J-aggregation—all of which are essential for increasing device efficiency. Additionally, the study discovered that P1TI displayed greater crystallinity whereas P3HT displayed a larger Stokes shift, suggesting increased disorder in the excited states of P3HT. This implies that P1TI might work better in applications that benefit from lower reorganization energy. These findings provide important information about how to modify solvent conditions and additives to regulate aggregation behavior, which optimizes material characteristics for organic electron.

Chapter 1

INTRODUCTION

1.1 Background

1.1.1 Organic Solar Cells and Their Development

Due to its low cost of manufacture and potential applications in the rapidly expanding field of flexible electronics, organic solar cells (OSCs) have garnered the interest of a large number of researchers worldwide [1]. Power conversion efficiency (PCE) of these devices has often been reported above 10 % [2]. Because of ongoing study and advancements in technology, the field of organic solar cells (OSCs) is always evolving. The potential for cost-effective and sustainable solar energy conversion offered by organic solar cells (OSCs) has attracted a lot of researchers to this field [3]. Other factors that contribute to this promise include the materials' availability, tenability, low cost, and simple production processes. Additionally, they are a strong contender for the quickly expanding flexible electronics sector because of their mechanical flexibility and light weight. In single-junction devices, OSCs' power conversion efficiency (PCE) has surpassed 18%, while in multi-junction devices, it has exceeded 17% [4].

OSCs, have a long history that has seen numerous breakthroughs and important turning points. The history of OSCs extends back several decades, with key milestones and breakthroughs along the way. The discovery of photoconductivity in organic materials, such as pigments and dyes, which produced electricity when exposed to light, in the 1960s marked the beginning of the breakthrough in OSCs [5–7]. After this discovery, conductive polymers were used to create OSCs and light-emitting diodes. Later, in the 1980s, [8] developed the bulk heterojunction (BHJ) concept as an effective means of preventing electron-hole recombination in organic semiconductors, hence improving the performance of OSCs. The basic idea behind the BHJ concept is combining two distinct organic materials with varying electronegativity to increase the active layer's donor-acceptor polymer interfacial area, which in turn improves exciton

free charges thereby boosting the efficiency of organic photovoltaic devices.

1.2 Milestones in Organic Solar Cells

The development of organic solar cells (OSCs) began in the 1980s and 1990s, with early research focused on using conjugated polymers such as polyacetylene as the active material. Although the initial devices demonstrated only modest efficiencies, they revealed the potential of organic materials for solar energy conversion. A significant breakthrough came with the discovery of photoconductivity in organic compounds, including organic pigments, which underscored the feasibility of OSCs. These advancements were driven by the synthesis of novel conjugated polymers with improved electronic properties, as well as progress in device fabrication techniques. The combination of material innovation and enhanced fabrication processes laid the foundation for continued improvements in OSC efficiency and stability, positioning organic solar cells as a promising alternative to traditional photovoltaic technologies[9].

1.3 Charge Transfer and Aggregation Effects

Some of the success stories in these significant increases include molecular structure optimization to make polymers with suitable energetics to promote charge transfer, high open circuit voltage, and broad absorption spectra to harvest the near-infrared part of the solar spectrum [10]. Low band gap polymers are typically created by copolymerization, which combines electron-rich donor (D) units with electron-deficient acceptor (A) units. The selection of matching moieties during synthesis dictates the hybridization of donor-acceptor (D-A) copolymers.

When small-molecule chromophores assemble in the solid state, they often form H-type or J-type aggregates, contingent upon the relative alignment of the transition dipole moments on adjacent molecules. Molecules primarily stack face-to-face in an H-aggregate, whereas head-to-tail stacking predominates in J-aggregate formation. The energy of the excited states and the oscillator strengths of the transitions from the ground state to these states are significantly affected by the creation of such aggregates. Consequently, optical absorption and the photoluminescence spectra can be significantly changed by H- and J-aggregation[11].

It is interesting to assemble one type of molecule in several packing modes in order to advance our knowledge of how molecular packing affects photovoltaic performance. Over the past few decades, research interest in polymer-based electronics has grown. This progress is significantly influenced by its low-cost potential as well as new applications like flexible electronic displays. Despite the fact that

some applications have been established with success, a wider application still necessitates a deeper comprehension of the impact of polymer arrangement on the device's electronic properties[12].

1.4 Intra and Inter-Chain Transport Mechanisms

All polymer-based devices, including transistors, organic light-emitting diodes, and organic solar cells, must improve charge carrier movement towards the electrodes. Charge transfer occurs either along the polymer backbone (intra-chain transport) or across π-orbitals connecting neighboring polymer chains in conjugated polymers (inter-chain transport). While the orientation of the polymer backbone mostly influences intra-chain transport, inter-chain transport is also crucial for device performance[13].

When H-aggregates are formed, their photoluminescence is quenched, and their major absorption peak is hypsochromic (blue-shifted) in comparison to that of their isolated monomer. They can be identified by the fact that they have two or more chromophores aligned face-to-face, meaning that the stacking direction is roughly perpendicular to the molecular plane. In J-aggregates, on the other hand, their photoluminescence is preserved, and the absorption spectrum is bathochromically (red-shifted) shifted in comparison to that of its isolated monomer. Furthermore, their chromophores are positioned side-by-side and roughly parallel to the molecular plane[14].

Both the relative alignment of the transition dipoles of the aggregated chromophores and their continuous spatial connectivity contribute to the red/blue shift of the primary absorption peak. Due to the fact that polymer π-layers are typically two-dimensional systems, their electronic excitations can delocalize both intermolecularly (J-aggregates) and intramolecularly (H-aggregates) along the polymer chain. Electronic transitions between the ground state and the lowest energy level of the vibrational excited state (0-0 transition) are not allowed in coupled H-type systems due to symmetry constraints. As a result, the absorption ratio of the 0-0 to 0-1 transition (0-0/0-1) is less than 1, which results in weaker emission at the 0-0 transition in its emission and H-aggregation. In contrast, the 0-0 transition is strongly permitted in J-type aggregates, which causes an absorption ratio at the 0-0/0-1 transition to be greater than 1 in both the absorption and emission spectra of J-aggregates[15].

1.5 Motivation of the Study

Science and technology are vast topics that encompass a wide range of specialties in any industry of technology specialists. Organic semiconductors are made from abundant materials such as plants. This is less expensive and simpler to produce and deposit on flexible substrates 3 customized to re-

quired electrical and optical small-molecule compounds are important for current commercial products such as photo conductors in copiers and laser printers, light-emitting and conducting layers in TV and smart phone displays, field-effect transistors (FET), organic solar cells (OSCs), sensors, and so on [16]. Indeed, advancements in organic electronics conjugated polymers offer greater possibilities for film formation and mechanical qualities than tiny molecules.

1.6 Isoindigo-based Copolymers and Why They are Important

Isoindigo is an organic compound derived from indigo, a well-known natural dye. Structurally, isoindigo consists of two indole units connected by a double bond, with additional carbonyl groups on each side of the molecule. This configuration gives isoindigo strong electron-accepting properties, making it valuable in the development of semiconducting materials, especially for applications in organic electronics such as solar cells and field-effect transistors. Isoindigo's planar structure enables efficient π-π stacking, which enhances charge transport, while its photostability makes it well-suited for optoelectronic devices[17].

An isoindigo-based copolymer refers to a polymer where isoindigo is one of the monomers, typically combined with an electron-donating monomer to create a donor-acceptor copolymer. These copolymers are designed to optimize electronic and optical properties, crucial for devices like organic solar cells and OLEDs[18, 19]. The combination of electron-donating and electron-accepting units allows fine-tuning of the copolymer's energy levels, enhancing light absorption and charge transport. Such copolymers are especially valued for their ability to absorb light in the visible and near-infrared regions and for their improved charge separation, making them key materials in advanced electronic application[20].

1.7 Statement of the Problem

The photo-physical properties and charge generation processes in donor-acceptor (D-A) copolymers play a critical role in their performance for various applications, including those involving P3HT and P1TI polymers[21]. Despite the potential of aggregation in enhancing these properties, there remains a lack of comprehensive understanding of how aggregation affects the optical and electronic behavior of such copolymers. Specifically, the mechanisms governing H and J aggregation in P3HT and P1TI, and their implications for material performance, have not been fully explored. This gap in knowledge limits the ability to optimize these materials for use in organic electronics[22].

This study seeks to address these gaps by investigating the effects of H and J aggregation on the optical properties of P3HT and P1TI in different solvent conditions. By understanding the underlying parameters of aggregation in copolymers, this research will offer insights into minimizing undesirable effects and improving material performance through experimental analysis. The findings of this work will contribute to the development of more efficient D-A copolymers and advance their applications in organic electronic devices[23].

1.8 Objectives

1.8.1 General Objective

To understand and identify the H and J aggregation properties on the photophysics of two selected co-polymers, namely P3HT and P1TI.

1.8.2 Specific Objectives

1. To determine the Optical properties of P3HT and P1TI in o-DCB.
2. To determine the effect of solvent (o-DCB and CF) in the polymers P3HT and P1TI.
3. To determine the effect of additive DIO in the polymers P3HT and P1TI.

1.9 Organization of the Thesis

This thesis is organized into five chapters, each of which addresses a specific aspect of the research on the aggregation-induced photophysics of isoindigo-based copolymers, specifically focusing on P3HT and P1TI. Below is an overview of each chapter:

Chapter 1 provides a comprehensive background on organic solar cells, highlighting their development and milestones. It covers key topics such as charge transfer mechanisms and the importance of aggregation in influencing these processes. Additionally, it details the motivation behind the study and explains the relevance of isoindigo-based copolymers in the context of organic electronics. The chapter concludes with the statement of the problem, which outlines the gaps in knowledge regarding H and J aggregation, and presents the general and specific objectives of the research.

Chapter 2 presents a thorough review of the literature related to organic semiconductors and copolymers, with a specific focus on isoindigo-based copolymers. It examines the photophysics of aggregates,

particularly the formation of H and J aggregates, and their photophysical properties. The role of various factors such as solvents, additives, and annealing in influencing aggregation is critically discussed. The chapter concludes with an overview of how absorption and photoluminescence peak positions are determined in polymeric materials.

In Chapter 3, the materials and experimental procedures used in the study are outlined in detail. The chapter begins by describing the polymer systems and solvents used, followed by the preparation of thin films on glass substrates. The methods for measuring UV-Visible and photoluminescence spectra are also discussed, as well as the principles underlying the absorbance and photoluminescence spectroscopy techniques used to analyze the samples.

Chapter 4 presents and analyzes the experimental results, focusing on the optical properties of P3HT and P1TI in different solvent conditions, with and without the addition of high boiling point additives. The chapter also explores the effects of solvent and DIO on the aggregation properties of the copolymers, detailing the impact of these factors on the photophysical behavior of the materials. A comparison of the effects of different treatments on the Stokes shift and photoluminescence is provided, offering insights into how aggregation influences material performance in optoelectronic applications.

Chapter 5 summarizes the key findings of the research, providing a concise conclusion on how H and J aggregation affect the optical properties and charge transport mechanisms in P3HT and P1TI. Recommendations are made regarding the choice of solvents, additives, and annealing processes to optimize the performance of these materials in organic electronics. The chapter ends by suggesting future research directions to further explore the relationship between aggregation and material properties.

Chapter 2

LITERATURE REVIEW

2.1 Overview of Organic Semiconductors

Organic semiconductors (OSCs) are an emerging class of materials with great potential in electronics due to their flexibility, lightweight nature, and tunability. An organic semiconductor is any material that possesses semiconductor qualities and has an electrical conductivity that falls between that of regular metals (conductors) and non-metals (insulating compounds). Solids made of heteroatoms including oxygen, nitrogen, sulfur, and hydrocarbons (carbon and hydrogen) are known as organic semiconductors. They can be found as thin, amorphous sheets and as molecular crystals [3, 24]. They are being investigated as an alternative to more traditional materials such as silicon, for the fabrication of different types of electronic devices. These materials have the advantages of flexibility, light weight, and quick and inexpensive device production processes. Their flexibility further allows for the development of rollable or foldable screens [25].

We examine a few small-molecule organic semiconductors in this thesis in light of their potential use in thin-film transistors and solar cells, among other technologies [26]. OSCs are particularly advantageous in applications like flexible electronics, organic photovoltaics (OPVs), and organic light-emitting diodes (OLEDs), where these properties allow for new innovations. In flexible electronics, organic semiconductors are valued for their ability to maintain electrical performance while undergoing mechanical deformation, enabling wearable technologies and foldable displays [27]. For OPVs, the tunability of OSCs helps optimize the light absorption spectrum, and their low-cost production methods make them promising for large-scale solar energy solutions. Moreover, the ability to produce semi-transparent and flexible solar panels offers integration into non-traditional surfaces, from windows to textiles. In OLEDs, OSCs enable energy-efficient, lightweight, and ultra-thin displays with superior color rendering, which are already prevalent in smartphones and televisions.

In general, organic semiconductors represent a key material class in advancing flexible electronics, energy-efficient OPVs, and the next generation of OLED displays, where flexibility, efficiency, and cost-effectiveness are prioritized. Over the last three to four decades, conjugated polymers, or organic semiconductors, have emerged as a promising conducting material for photovoltaic applications[28]. The special characteristic of organic semiconductors is their ability to blend polymers. This gives rise to an infinite possibility of customizing their mechanical, optical, and electrical characteristics. It also provides a broad range of uses for organic semiconductors in displays, organic field effect transistors, light emitting diodes, and OSCs. Because organic semiconductors have a high extinction coefficient, photons can be efficiently absorbed in a layer of. This offers countless opportunities to customize their mechanical, optical, and electrical characteristics. Additionally, it offers up a wide range of applications for organic semiconductors in displays, OSCs, organic field effect transistors, and light-emitting diodes. Because of their high extinction coefficient, organic semiconductors allow for the effective absorption of photons in a merely a few hundred nanometers thick layer. As a result, OSCs are flexible and light[29]. Typically, low-cost solution process able methods like spin coating or evaporation processing are used to create OSCs. The recent advancement in fabrication of OSCs in the view of mass manufacturing is headed towards roll-to-roll printing technology. This method is comparable to a basic inkjet print. Roll-to-roll printing of OSCs requires a flexible substrate. In addition to their mechanical adaptability, their variety of colors presents engineers with a special chance to create application-specific designs. Utilizing their mechanical flexibility and variety of hues, German researchers have recently demonstrated the potential for self-powered gadgets such as solar cell-integrated smart eyewear [30].

2.2 Copolymers

Copolymers, formed by polymerizing two or more different monomer units, offer enhanced versatility in material properties compared to homopolymers[31]. Their unique ability to combine the characteristics of various monomers allows for fine-tuning of mechanical, thermal, and chemical properties, making them highly adaptable for specific applications. For instance, copolymers can exhibit improved elasticity, toughness, or solubility by adjusting the composition and arrangement of their monomers, which can be in random, alternating, block, or graft configurations[32]. This adaptability has made copolymers essential in various industries, including packaging, textiles, automotive, and healthcare, where materials need to meet specific performance criteria. In advanced applications like organic electronics, donor-acceptor (D-A) copolymers play a crucial role, as they allow precise control over optoelectronic properties, leading to efficient charge transport and light absorption. Isoindigo-based copolymers, for example, are widely

used in organic solar cells and field-effect transistors due to their tunable electronic properties. The ability to manipulate copolymer structures opens new pathways for creating materials that can meet the evolving demands of technology and industry[**anies2020structurally**].

Figure 2.1: Different types of polymers: 1) homopolymer 2) alternating copolymer 3) random copolymer 4) block copolymer 5) graft copolymer.This diagram is taken from Wikipedia

2.3 Isoindigo Dye Incorporated Copolymers

Isoindigo copolymers are a class of organic semiconducting materials derived from the isoindigo molecule, which is a derivative of indigo dye known for its strong electron-accepting characteristics and a planar structure conducive to π-π stacking[33]. Isoindigo copolymers are created by combining isoindigo units with various donor monomers through covalent bonding, forming donor-acceptor (D-A) architectures. These copolymers possess unique electronic and optical properties, such as a low band gap, high charge mobility, and tunable absorption spectra, making them suitable for use in organic electronics[34]. The donor-acceptor architecture is essential because the isoindigo unit, acting as the electron acceptor, pairs with electron-donating units (such as thiophene or benzodithiophene) to enhance charge separation and transport[35]. This D-A structure facilitates efficient charge mobility in devices like organic solar cells (OSCs), organic field-effect transistors (OFETs), and organic light-emitting diodes (OLEDs). Additionally, the planar structure of isoindigo enables strong π-π interactions, which further improves the material's electrical conductivity and stability. Isoindigo copolymers are particularly valuable in organic photovoltaics due to their ability to absorb light in the visible and near-infrared regions, and they can be easily modified to adjust their electronic properties for specific applications[36]. The versatility and tunability of isoindigo copolymers make them promising candidates for next-generation flexible, lightweight, and low-cost electronic devices such as flexible displays, solar panels, and sensors.

Isoindigo-based copolymers have shown promising applications in various fields of organic electronics due to their tunable optoelectronic properties, charge mobility, and strong π-conjugation. A significant application is in organic solar cells (OSCs), where isoindigo copolymers are used as donor materials in the active layer, achieving high open-circuit voltages and power conversion efficiencies. For instance, modifying the isoindigo structure with thiophene bridges has improved the photovoltaic performance of organic solar cells, achieving higher efficiencies [37]. Furthermore, isoindigo-based copolymers have been employed in non-fullerene OSCs, leading to efficiencies exceeding 12%, showcasing the material's versatility and high performance in advanced photovoltaic technologies [38]. These copolymers are also used in organic thin-film transistors (OTFTs), providing both ambipolar and n-channel properties, which is essential for developing low-power and flexible electronic devices [39]. Additionally, they find applications in organic light-emitting electrochemical cells (OLECs), where they serve as active materials, enabling efficient electron/hole doping and light emission [40].

2.4 Photophysics of Aggregates

The photophysics of aggregates plays a crucial role in understanding the behavior of organic materials in condensed states, such as conjugated polymers and molecular aggregates. In conjugated polymer aggregates, the mesoscopic morphology strongly influences optoelectronic properties, which are essential for the performance of polymer-based optoelectronics like organic solar cells and light-emitting devices. Single-molecule fluorescence techniques have been employed to examine how aggregation affects the photophysical properties, offering insights into electronic coupling and energy transfer processes [41]. In molecular aggregates, particularly centrosymmetric systems, group theory analysis reveals that symmetry can dictate optical selection rules and impact transitions between singlet and triplet states, which are vital for understanding ultralong organic phosphorescence [42]. The behavior of specific dyes, such as BODIPY aggregates, demonstrates how both steady and excited-state interactions can vary depending on the environment, such as in solvent mixtures or monolayer compression, which affects the fluorescence lifetimes and aggregation-induced emissions [43].

Early in the 1960s, Kasha et al. [45] created a model to explain why conjugated small molecules and conjugated polymer chromophores differed in their photo physical characteristics when they aggregated in solution or in the solid state. They also discovered a connection between the aggregates' morphology and optical characteristics (such as absorption and photoluminescence or fluorescence). Chromophores can form two different forms of aggregates: J-aggregates and H-aggregates, depending on the orientation of the transition dipole moments between nearby molecules. Aggregation can be induced by increasing the concentration of fluoresces material in a solution or by introducing poor solvents to the

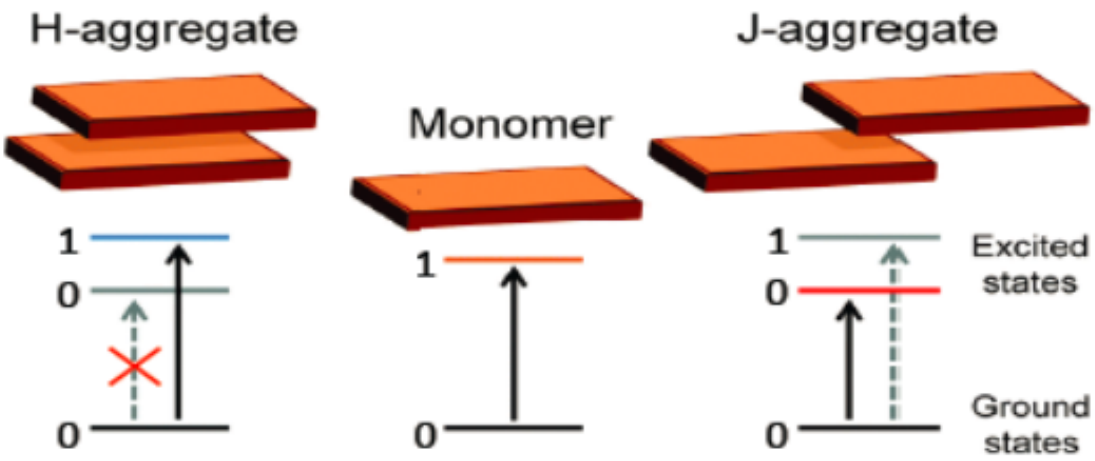

Figure 2.2: Energy diagrams of molecular aggregates and monomers showing exciton interactions. The diagram illustrates the difference between H-aggregate, monomer, and J-aggregate systems. For the monomer, excitation happens from the ground state (0) to the excited state (1) without any shift. In H-aggregates, the excited state energy is higher due to exciton coupling, leading to a blue shift (shown by the blue line), while transitions to lower energy states are forbidden. In J-aggregates, exciton coupling causes a red shift in the excited states (shown by the red line), allowing a transition to lower energy states.[44]

polymers solution. In contrast to the monomer, an H-aggregate exhibits a side-by-side arrangement of the chromophores, resulting in a positive Coulomb coupling (Jc) and a blue-shifted absorption peak. On the other hand, a J-aggregate indicates a head-to-tail arrangement of the chromophores, leading to a negative Jc and red-shifted absorption. Kasha's research revealed that polymers display two primary forms of molecular packing [46, 47].

In polymers, a band of an intra-chain exciton of the Wannier-Mott type is the first electronically excited state. However, due to interactions with nearby polymer chains, aggregated polymer films also contain a Frenkel type inter-chain exciton that is important for the charge dynamics of organic electrical devices. Polymers in which the donor and acceptor units alternate: Copolymers: Depending on their electron affinity, polymers can be categorized as either electron-donating or electron-accepting. These are comparable to inorganic semiconductors of the p and n types, respectively. A D-A copolymer can be created by coupling an electron-rich donor (D) polymer and an electron-deficient acceptor (A) polymer[48].

When H-aggregates come together, their photoluminescence is extinguished and their primary absorption peak is hypsochromically (blue-shifted) in relation to that of its isolated monomer. Their defining feature is the arrangement of two or more chromophores face-to-face, meaning that the stacking direction is roughly perpendicular to the molecular plane. On the other hand, the photoluminescence of J-aggregates is preserved and their absorption spectrum is bathochromic ally (red-shifted) in relation to that of their isolated monomer[49]. In addition, their chromophores are arranged in a direc-

tion that is approximately parallel to the 14 molecular planes, side by side. Two causes contribute to the primary absorption peak's red/blue shift: two things: (I) the aggregated chromophores' transition dipoles' relative alignment; and (ii) their constant spatial connection. Since polymer π-layers are usually two-dimensional systems, their electronic excitations can delocalize both along the polymer chain intramolecular (J-aggregates) and between chains intermolecular (H-aggregates). In coupled H-type systems, electronic transitions between the ground state and the lowest energy level of the vibrational excited state (0-0 transition) are forbidden by symmetry, and therefore the absorption ratio of the 0-0 to 0-1 (0-0/0-1) transition is less than 1, leading to weakened emission at its 0-0 transition in its emission[50]. On the contrary, in J-type aggregates the 0-0 transition is strongly allowed, which results in an absorption ratio at the 0-0/0-1 transition above 1 in both the absorption and emission spectra [51].

Converged polymer research has garnered attention from the scientific community because of its many applications, including photovoltaics, field-effect transistors, and organic light-emitting diodes (OLEDs) [52–55]. Recent years have seen a significant increase in the performance of OLEDs, which has led to their introduction into the market. Meanwhile, organic solar cells (OSCs), whose power conversion efficiencies have recently been pushed to about 20%, are making steady progress toward commercialization. [56–58]. Near-neighbor interactions in an aggregate may have a substantial impact on the photo physics of the polymers, changing the application of a particular polymer from being better suited for OSCs than for OLEDs, or vice versa. In particular, the polymer packing for OSCs should optimize charge separation and transport, whereas the packing shape for OLEDs should promote electroluminescence by promoting electron recombination.

Using non-covalent intramolecular interactions to create a conformational lock in the conjugated backbone is a relatively recent technique for altering the band gap energy of conjugated polymers. The device shape, polymer size domains, and structural arrangement/conformation of polymer chains can all be adjusted by these effects, which can then have an impact on the effectiveness of charge transport and exciton dissociation [59].

In two-dimensional π-stacked lamellar structures, regioregular poly (3-hexylthiophene) (rrP3HT) self-organizes in thin films [60, 61]. Certain polymer properties and thin-film manufacturing parameters have a sensitive impact on the level of order inside and around these supramolecular structures [62]. Device performance is then significantly impacted by these. Here, we employ linear absorption spectroscopy as a straightforward tool to examine how processing parameters affect the microstructure of thin films. A weakly interacting H-aggregate model provides a comprehensive explanation for the absorption spectra of rrP3HT thin films [63, 64]. This model may be used to analyze the absorption spectra, yielding

quantitative estimates of the degree of excitonic coupling within the film as well as the fraction of the film composed of aggregates, which was recently measured using several methods [65, 66].

2.5 Photophyiscal Properties of H and J aggregation

Leyi Tang et' al have investigated "Fluorine substitution for aggregation transformation and exciton dissociation acceleration in non-fused electron acceptors" [67]. They have concluded that fluorine substitution plays a critical role in transforming aggregation behavior and enhancing exciton dissociation in non-fused electron acceptors. The introduction of fluorine significantly improved molecular packing, which facilitated more efficient charge transport and exciton dissociation, essential processes for improving the performance of organic photovoltaic devices. By optimizing the molecular interactions within the material, the study demonstrated that fluorine substitution can lead to enhanced optoelectronic properties, thereby advancing the design of non-fused electron acceptors for next-generation organic solar cells [67].

Qiaoqiao Zhao et'al [68] have investigated "H- and J-aggregation of conjugated small molecules in organic solar cells". In their study, Qiaoqiao Zhao et al. (2016) investigated the balance between H- and J-aggregation in small molecule organic solar cells, focusing on how these aggregates impact photovoltaic efficiency. They concluded that while J-aggregation leads to the formation of more excitons due to its narrower bandgap and higher photocurrent, H-aggregation provides a stronger driving force for exciton dissociation, essential for charge separation. In their work on the p-DTS(FBTTh2)2/PC70BM blend system, they observed that the material's crystallinity was low, and it primarily formed J-aggregates. However, by applying solvent vapor annealing (SVA), they were able to increase H-aggregation, improving the material's crystallinity and resulting in a more favorable H/J aggregation ratio. This adjustment enhanced the power conversion efficiency (PCE) from 2.64% to 6.63%, demonstrating that a balance between H- and J-aggregation is crucial for optimizing the performance of organic solar cells[69]. The study highlights the importance of controlling molecular packing and aggregation to achieve efficient exciton dissociation and charge transport in organic photovoltaic devices.

In their study, Chauhan et al. (2024) investigated the aggregation-induced strong photoluminescence in large-area C8BTBT thin films at room temperature. The researchers concluded that the photophysical behavior of C8BTBT films is strongly dependent on film thickness, with thicker films exhibiting different photoluminescence characteristics compared to thinner films[70]. Their findings revealed that aggregation, including J- and H-type aggregation, plays a significant role in influencing the ultraviolet (UV) emission spectra of the films. The study also showed that highly crystalline C8BTBT films, confirmed

through grazing incidence X-ray diffraction, exhibit increased crystal coherence length with film thickness, which in turn affects their optical absorption and emission properties. The presence of defects and aggregation behavior in these films impacts their UV emissions, making these findings crucial for optimizing C8BTBT thin films for potential use in low-cost, flexible optoelectronic and photonic devices [71].

Achieving both high mobility and strong fluorescence in organic semiconductor materials (OSCs) remains a significant challenge, as materials with high mobility often exhibit weak fluorescence. However, both properties are crucial for optimizing the efficiency of optoelectronic devices. One key factor that influences the performance of OSCs is the molecular aggregation type within the active layer, alongside the chemical structure of donor and acceptor molecules and the nanoscale morphology of the layer[72]. The two primary forms of molecular aggregation—H- and J-aggregation—result from $\pi - \pi$ interactions between conjugated units, where H-aggregates stack face-to-face and J-aggregates stack head-to-tail. The angle between the conjugated plane and the aggregation direction is critical in distinguishing these aggregates. H-aggregates, characterized by angles greater than 54.7°, lead to blue-shifted absorption spectra due to their higher energy levels, whereas J-aggregates, with angles below 54.7°, exhibit red-shifted absorption and are associated with stronger fluorescence due to lower energy levels. The type of aggregation affects both charge mobility and optical properties, making it essential to consider how different materials—whether donor or acceptor—interact within these aggregations to optimize performance. Comparative studies investigating how H- and J-aggregates impact OSC performance, especially in terms of balancing mobility and fluorescence, are limited but necessary for advancing the development of efficient optoelectronic devices[73].

2.6 Factors Influencing the forming of H- and J-aggregation in Thin Film

The formation of H- and J-aggregations in thin films is influenced by various factors, including molecular structure, processing conditions, solvent selection, and film morphology. H- and J-aggregations result from π-π interactions between conjugated units, where H-aggregates stack face-to-face and exhibit blue-shifted absorption, while J-aggregates stack head-to-tail, leading to red-shifted absorption[74]. The ratio of H- to J-aggregates can be controlled by manipulating solvent properties, such as boiling point, and by adding processing additives, which can selectively influence the dissolution of side chains or control molecular motion. For example, in DTS(PTTh$_2$)$_2$/PC$_{70}$BM systems, the H/J aggregation ratio can be tuned using additives like diiodoalkanes, which significantly affect the power conversion efficiency (PCE) of organic solar cells, as a balanced aggregation is required to optimize light absorption and exciton

dissociation [75]. Additionally, solvent choice plays a pivotal role in determining aggregation behavior, as demonstrated by squaraine dyes where H- and J-aggregates formed under different solvents showed distinct optical and electrical properties, with J-aggregates contributing more to photocurrent in organic photovoltaics [76]. Moreover, bulky side groups or specific chemical modifications can induce or switch between H- and J-aggregates in solid-state films, further influencing the electronic and optical behaviors of the material [77].

2.6.1 The Role of the Solvents

Solvents play a crucial role in influencing the formation of H- and J-aggregations in thin films, primarily by affecting molecular organization and crystallinity during the film formation process. The solvent's boiling point, polarity, and ability to dissolve different molecular components can determine whether H- or J-aggregates dominate. For instance, solvents with a high boiling point allow for slower evaporation, giving molecules more time to self-organize and form either H- or J-aggregates based on their structural characteristics[78]. In the case of squaraine dyes, for example, the choice of solvent directly influences the type of aggregation formed. H-aggregates, which exhibit face-to-face stacking, tend to form in polar solvents, leading to blue-shifted absorption spectra, while J-aggregates with head-to-tail stacking form in solvents that promote stronger π-π interactions, resulting in red-shifted absorption and enhanced photocurrent generation in photovoltaic applications [76]. Furthermore, additives and processing solvents can selectively dissolve different parts of the polymer or molecule, leading to fine-tuning of the H/J aggregation ratio, which is crucial for optimizing light absorption and charge separation in organic solar cells [75]. Therefore, by carefully selecting the solvent or adding specific solvent additives, the balance between H- and J-aggregates can be controlled to enhance device performance.

2.6.2 The Role of Additives

Additives have a significant impact on the ratio of H- and J-aggregates in organic solar cells (OSCs) by influencing the molecular packing, crystallinity, and phase separation of donor and acceptor materials within the active layer. These additives alter the self-organization of molecules during the film formation process, thereby tuning the relative content of H- and J-aggregates. For instance, in the DTS($PTTh_2$)$_2$/PC_{70}BM system, adding specific additives such as 1,6-diiodohexane (DIH) and 1,8-diiodooctane (DIO) can selectively dissolve side chains, increasing the ratio of H-aggregates[79]. This promotes improved crystallinity and molecular alignment, enhancing exciton dissociation and charge transport. H-aggregates, with their face-to-face stacking, contribute to a stronger driving force for exciton dissociation due to their higher energy levels. On the other hand, J-aggregates, which have head-to-tail stacking, favor exciton formation due to their lower energy requirements for excitation, contributing to more efficient

light absorption.

2.6.3 The Role of Annealing

Thermal treatment plays a crucial role in enhancing the optoelectronic properties of isoindigo-based copolymers by influencing their molecular packing, crystallinity, and phase transitions. When subjected to thermal annealing, the copolymer chains gain enough mobility to rearrange into more ordered structures, leading to improved π-π stacking and enhanced crystallinity[80]. This increased order facilitates better charge transport and exciton diffusion, essential for higher performance in organic electronics such as organic solar cells (OSCs) and organic field-effect transistors (OFETs). Specifically, thermal treatment can help optimize the degree of aggregation, which in turn affects light absorption and fluorescence emission[81]. For example, increased crystallinity due to thermal annealing typically leads to stronger absorption in the visible to near-infrared regions, which is beneficial for photovoltaic applications. Moreover, the mobility of charge carriers, such as electrons and holes, is enhanced due to improved interchain coupling, resulting in higher field-effect mobilities in OFETs. However, excessive thermal treatment can also lead to over-aggregation, which may result in reduced fluorescence due to non-radiative recombination processes or exciton quenching. Thus, carefully controlled thermal treatment is essential to achieve a balance between crystallinity and optimal optoelectronic performance in isoindigo-based copolymers [82].

Optimizing the optoelectronic properties of isoindigo-based materials through thermal processing involves careful control of annealing temperature, time, and the environment in which the treatment occurs. Thermal annealing typically improves molecular packing and crystallinity, which are key factors in enhancing charge transport and light absorption. For isoindigo-based copolymers, the ideal annealing temperature usually ranges between 150℃ and 200℃, depending on the specific molecular structure and the side chains attached to the isoindigo unit. This temperature range allows for sufficient chain mobility, enabling the molecules to organize into more ordered $\pi - \pi$ stacking arrangements, improving charge carrier mobility and reducing energetic disorder[83].

The duration of annealing is equally important; too short a treatment may not allow the material to reach an optimal degree of crystallinity, while overly long annealing can lead to over-aggregation or phase separation, which may quench photoluminescence or hinder exciton diffusion. Typically, annealing times of 10 to 30 minutes are found to strike a balance, allowing materials to reach a well-ordered structure without inducing detrimental aggregation[84]. The atmosphere in which annealing is conducted, whether under inert gas (e.g., nitrogen) or vacuum, also influences the results, as it can prevent oxidation or degradation of the copolymer, further preserving its electronic properties.

Controlling these parameters—temperature, time, and atmosphere—optimizes the morphology of the active layer, leading to improved performance in devices like organic solar cells (OSCs) and organic field-effect transistors (OFETs), where enhanced crystallinity and balanced aggregation are crucial for achieving high power conversion efficiencies and charge mobility[85].

2.7 Absorption and Photo-luminescence Peak Positions in Polymeric Materials

When small-molecule chromophores aggregate in the solid state, they typically form either H-type or J-type aggregates based on the relative orientation of their transition dipole moments. H-aggregates arise from face-to-face stacking of molecules, resulting in a blue-shift (hypsochromic shift) of the absorption spectrum, while J-aggregates, which have head-to-tail stacking, exhibit a red-shift (bathochromic shift) in absorption[86]. The formation of these aggregates significantly alters the energy levels and oscillator strengths of the transitions, affecting both optical absorption and photoluminescence (PL) spectra. In H-aggregates, photoluminescence is often quenched due to the formation of non-radiative states, whereas J-aggregates retain their photoluminescence with a red-shifted emission. These aggregation types are particularly important in the study of polymer-based electronics, such as organic solar cells (OSCs), where the molecular packing can influence charge transport and exciton dynamics[87]. For instance, in OSCs, H-aggregates might promote better exciton dissociation due to their higher energy levels, while J-aggregates facilitate exciton generation due to lower excitation energies. The balance between these two forms of aggregation is crucial for optimizing device performance by enhancing charge carrier mobility and improving light absorption [88, 89].

In the context of polymeric materials, the absorption and photoluminescence (PL) peak positions provide crucial insights into the material's optical properties, particularly for applications in solar cells, light-emitting diodes (LEDs), and other optoelectronic devices. The absorption peak position, typically determined via UV-Vis spectroscopy, indicates the wavelength at which a polymer absorbs the most light. This peak corresponds to the energy required to excite an electron from the highest occupied molecular orbital (HOMO) to the lowest unoccupied molecular orbital (LUMO). For conjugated polymers, which have delocalized π-electrons, the absorption peak is often in the visible spectrum, making them ideal for applications requiring visible light absorption[91]. Photoluminescence occurs when excited electrons return to the ground state, emitting light, and the PL peak position represents the wavelength at which this emission occurs. Typically, photoluminescence is observed at longer wavelengths than absorption due to energy loss through non-radiative processes, a phenomenon known as the Stokes shift[92].

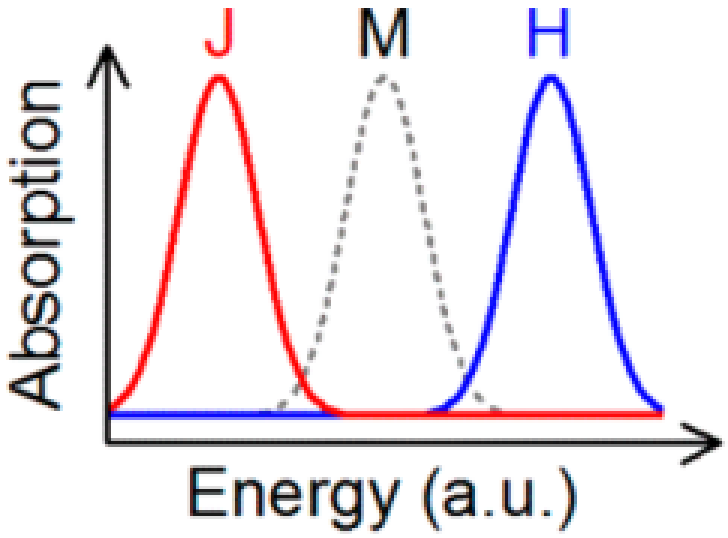

Figure 2.3: A typical absorption spectra of J-aggregates, monomers, and H-aggregates. The plot shows the absorption profiles where the monomer (M) exhibits an intermediate absorption peak, while H-aggregates (H) display a blue-shifted absorption, and J-aggregates (J) show a red-shifted absorption. The shifts arise due to different exciton couplings in the aggregates, with H-aggregates having higher energy absorption and J-aggregates having lower energy absorption compared to the monomer.This diagram is taken from literature [90]

These absorption and PL peak positions are essential for understanding a polymer's energy levels and excitonic behavior, which are critical for the efficiency of devices like organic solar cells. The difference in energy between the donor's HOMO and the acceptor's LUMO, which governs exciton dissociation and influences the open-circuit voltage (V_{oc}), is affected by the aggregation behavior of the materials, highlighting the importance of both H- and J-aggregates in optimizing device performance [75, 93]

Chapter 3

MATERIALS AND METHODS

3.1 Materials

The polymer system studied in this research consists of isoindigo (C16H10N2O2) as the acceptor moiety and various thiophene-based derivatives as the donor components, including thiophene (C4H4S), bi-thiophene (C8H6S2), and ter-thiophene (C12H8S3). These polymers were carefully synthesized and prepared for subsequent thin-film fabrication to ensure high-quality material with suitable optoelectronic properties.

Glass substrates were used as the base for film preparation. To ensure optimal surface cleanliness and reproducibility, the glass substrates were subjected to rigorous cleaning procedures. Initially, the substrates were washed in a sequence of organic solvents, such as chloroform (CF), followed by inorganic solvents, such as distilled water. The cleaned substrates were subsequently dried in an oven at 100℃ for one hour to remove any residual contaminants. This ensured a clean surface for subsequent polymer deposition.

To prepare the polymer solutions, 15 mg of the copolymers P3HT and P1TI were dissolved in 80 mL of different solvents, namely 1,2-dichlorobenzene (o-DCB), chloroform (CF), and cyclohexane (Chex). These solvents were chosen based on their refractive indices and polarity indices to optimize the solubility of the copolymers. Specifically, o-DCB has a refractive index (n) of 1.55 and a polarity index of 2.7; CF has n = 1.45 and a polarity index of 4.1; while Chex has n = 1.42 and a polarity index of 0.2. The use of multiple solvents allowed for the assessment of solvent effects on the optical properties of the resulting thin films. All chemicals and solvents used in this study were of analytical grade, and o-DCB was obtained from Sigma Aldrich to ensure high purity.

3.2 Methods

3.2.1 UV-Visible and Photoluminescence Measurements

UV-visible (UV/Vis) absorbance spectra were recorded using an Agilent Cary 5000 UV-Vis-NIR spectrometer equipped with an integrating sphere to accurately capture the light absorbed by the films in a diffuse environment. This configuration enabled more precise quantification of absorbance, especially for thin films with variable scattering properties.

For photoluminescence (PL) measurements, a Horiba Fluorolog-3 FL3-122 spectrofluorometer was used. The excitation source was a Xenon 450 W lamp, which provided a broad range of excitation wavelengths. Double-grating monochromators were employed in both excitation and emission light paths to achieve high spectral resolution and minimize stray light. Emission spectra were recorded at an angle of 25° relative to the normal of the substrate, with an excitation wavelength set to 530 nm. The detector used for PL was a Hamamatsu R928P photomultiplier tube, which provided high sensitivity across the ultraviolet and visible regions of the spectrum.

3.2.2 Optical Characterization

The absorption spectra of P3HT and P1TI thin films were recorded using a Perkin Elmer Lambda 19 UV-VIS/NIR spectrophotometer. The spectra were obtained to determine the optical band gap and to evaluate the light-harvesting capabilities of the polymers. Two different solvents, chloroform (CF) and 1,2-dichlorobenzene (o-DCB), were used to prepare the films, with polarity indices of 4.1 and 2.7, respectively, to assess the influence of solvent polarity on the optical properties. For photoluminescence (PL) studies, the copolymers' spectra were recorded using a JY Horiba Fluoromax-4 spectrofluorometer, and steady-state PL measurements were carried out at an excitation wavelength corresponding to the electronic transition, set at 580 nm, using an Edinburgh Instruments DS5 UV-Vis spectrophotometer.

3.3 Thin Film Preparation

Thin films were prepared by dissolving the copolymer in o-DCB and CF at a concentration of 15 mg/mL. The solutions were stirred at 120℃ for 30 minutes to ensure complete dissolution of the copolymer. Thin films were fabricated via spin-coating, which involved depositing the polymer solution onto pre-cleaned glass substrates. The spin-coating process was performed on a hot plate set at 85℃ to facilitate the even spreading of the solution across the substrate surface. The films were spin-coated using an Ossila CSS 05 spin coater at 1000 rpm for 50 seconds. Following spin-coating, the films were dried on a hot plate at 85℃ for 10 minutes to ensure the complete evaporation of the solvent, resulting in uniform thin

films.

The glass substrates used for spin-coating were prepared by cutting them into dimensions of 1.5 cm × 2 cm and cleaning them sequentially in soap, isopropanol, and acetone in an ultrasonic bath, each step lasting 10 minutes. After ultrasonic cleaning, the substrates were subjected to UV-ozone treatment for 30 minutes to improve their wettability and ensure better adhesion of the polymer films during spin coating.

3.4 Absorbance and Photoluminescence Working Principle

3.4.1 Absorbance Principle

Absorbance is a fundamental process involving the interaction of light with matter, where specific wavelengths of light are absorbed by a material. When light interacts with the polymer, photons of specific energies are absorbed, promoting electrons from the ground state to an excited state. The amount of light absorbed at each wavelength provides insights into the electronic transitions and energy levels within the material. The absorbed energy can be either dissipated as heat or used to induce chemical reactions, depending on the material properties and the experimental conditions.

3.4.2 Photoluminescence Spectroscopy Principle

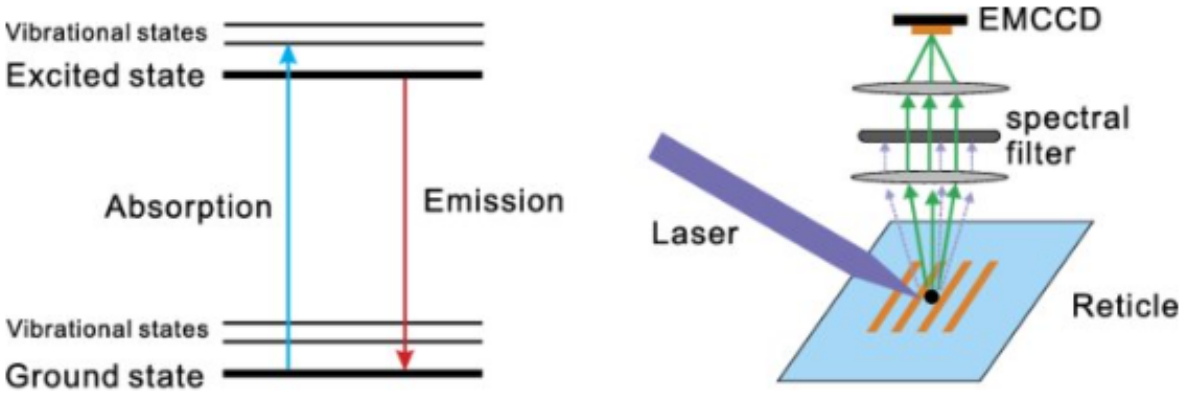

Figure 3.1: Schematic representation of photoluminescence in a material. The left side illustrates the electronic transitions where a photon is absorbed, promoting an electron from the ground state to an excited state, followed by emission of a photon as the electron returns to a lower energy state. The right side shows the experimental setup, where a laser excites the sample, and the emitted light passes through a spectral filter before being detected by an EMCCD camera. This diagram is taken from literature [94]

Photoluminescence (PL) spectroscopy is a powerful tool for investigating the optical properties of materials. In PL spectroscopy, the material is excited using a light source with energy greater than or equal

to the band gap of the material, causing electrons to transition to higher energy states. Upon relaxation, the excited electrons release photons, resulting in luminescence. The emitted light is collected and analyzed using a spectrometer, providing information about the optical band gap, defect states, and quantum efficiency of the material.

In this study, the PL setup included a laser with energy above the band gap to excite the polymer samples. The emitted light was collected using a spherical mirror system and directed to an optical fiber, which guided the light to a monochromator equipped with a diffraction grating. A liquid nitrogen-cooled InGaAs or Si photodiode array detector was used for sensitive detection of the emitted light. An extended-pass filter was used to remove the reflected excitation light, ensuring that only the emitted PL signal was recorded. Polarizers were also added when necessary to study the polarization properties of the emitted light, which can provide additional information about the alignment and symmetry of the polymer chains.

Chapter 4

RESULT AND DISCUSSION

4.1 Optical properties of P3HT and P1TI in ODCB

The absorption spectra of P3HT and P1TI was recorded in ODCB to understand the effect of isoindigo copolymerization on the optical properties of the two polymers. P3HT, the thiophene photopolymer, displayed one energy band, while distinct two energy bands were observed in P1TI due to the copolymerization. The absorption of both polymers has a vibronic feature in the high energy band corresponding to the $\pi \rightarrow \pi^*$ transition. Hence, we deconvoluted the peaks corresponding to the $\pi \rightarrow \pi^*$ transition using Gaussian fit as shown in Figure **??**. The two polymers revealed three vibronic peaks confirming their planar structure [95]. On the other hand, P1TI has an additional electronic transition at 420 nm corresponding to the $\pi \rightarrow \pi^*$ transition. In P3HT, the $\pi \rightarrow \pi^*$ transition is mainly due to the alternating single and double bonds in the backbone of the polymer. Similarly, the high-energy peak in P1TI corresponds to the $\pi \rightarrow \pi^*$ transition. Furthermore, the alternating donor and acceptor units in P1TI created an intramolecular charge transfer state (ICT), which is responsible for the transition corresponding to the band gap transition.

Table 4.1: Band gap of P3HT and P1TI in o-DCB

Co-polymer	**Λ onset (nm)**	**E_g (eV)**
P3HT _ o-DCB	660	1.88
P1TI _ o-DCB	775	1.6

The band gap of P3HT and P1TI in o-DCB is 1.88 eV and 1.6 eV, respectively, as our result indicates in Table 4.1. The isoindigo copolymerization of thiophene units evidently has reduced the band gap of the thiophene-based polymer, producing a low band gap polymer. This is essential to harness a large portion of the solar energy.

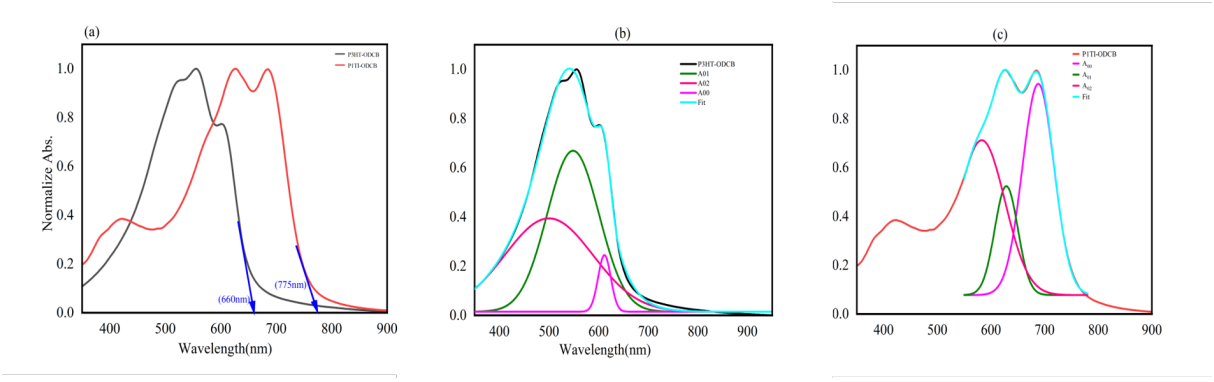

Figure 4.1: Absorbance of P3HT and P1TI in o-DCB: Normalized absorption spectra in different solvents and fitting results. (a) The absorption spectra of P3HT-ODCB (black) and PTTI-ODCB (red), showing the broad absorption in the visible region for both polymers with PTTI red-shifted compared to P3HT. (b) Decomposition of the absorption spectra of P3HT-ODCB into vibronic peaks A00 (green), A01 (magenta), A02 (purple), and the fitting curve (cyan). (c) Decomposition of the absorption spectra of PTTI-ODCB into vibronic peaks A00 (green), A01 (magenta), A02 (purple), and the fitting curve (cyan), showing more pronounced vibronic structures compared to P3HT.

The optical properties of the two polymers were further investigated using steady-state photoluminescence spectroscopy as shown in 4.2. The emission was collected by exciting the polymer films at their absorption maxima. As expected, P1TI revealed a red-shifted PL peaking at 804.06 nm, while the PL of P3HT peaks at 790.76 nm, consistent with their band gap. Furthermore, the PL spectra of the two polymers were fitted with two Gaussian curves, as shown in Figure 4.2. The PL of P3HT is predominantly from one relaxing channel, while P1TI has two dominant relaxation channels, as revealed by the two Gaussian curves. This confirms that the exciton relaxation in P3HT is predominantly through one channel, while P1TI has both intra-chain and interchain exciton relaxation channels. An exciton can be intra-chain or interchain when there is significant inter-chain interaction in films [96]. Hence, it can be concluded that P3HT has mainly intra-chain excitons, while P1TI exhibits both intra-chain and interchain excitons, confirming that good inter-chain interaction can be achieved through isoindigo copolymerization.

Table 4.2: Stokes shift of P3HT and P1TI in o-DCB

Co polymer	λ_{em} (nm)	λ_{abs} (nm)	**Stokes shift** ($\Delta\lambda$) (nm)
P3HT_o-DCB	733.94	611.74	122.2
P1TI_o-DCB	852.16	650.19	201.97

Upon excitation, the molecules undergo rapid conformational changes due to vibration, rotation, and translational motion, which induces a larger shift in emission energy compared to the absorption energy. This phenomenon is called the Stokes shift. The Stokes shift (Δ) is defined as: $\Delta = \lambda_{\text{Emission}} - \lambda_{\text{Absorbance}}$. The Stokes shift of P3HT and P1TI were found to be 122.20 nm and 201.97 nm, respectively. The larger shift in P1TI confirms a larger backbone conformation change upon excitation in the copolymer compared to P3HT.

4.2 Aggregation in P3HT and P1TI

Detailed photophysics that determine the aggregation of the polymers can be deduced from the ratio of the absorptions at the first (A_{00}) and the second (A_{01}) vibronic shoulders, as discussed by [97]. The $\pi \rightarrow \pi^*$ transition of P3HT and P1TI are fitted with Gaussian curves, as shown in Figure **??**, and the values of the vibronic transitions are summarized in Table 4.3.

Table 4.3: Absorption of P3HT and P1TI in o-DCB peak position

Transition Band	**P3HT_ o-DCB**		**P1TI_ o-DCB**	
	(nm)	Absorbance	(nm)	Absorbance
A_{00}	611.74	0.23	688.20	0.93
A_{01}	548.50	0.66	628.64	0.51
A_{00}/A_{01}		0.34		1.82

An H-aggregate is known to have a forbidden 00 transition, while a J-aggregate reveals a bright 00 transition, making the A_{00}/A_{01} ratio less than 1 in H-aggregates and greater than 1 in J-aggregates [98]. As shown in Table 4.3, P3HT and P1TI films prepared from o-DCB reveal A_{00}/A_{01} ratios of 0.34 and 1.82, respectively, confirming that P3HT adopts H-aggregation while P1TI adopts J-aggregation. The result with P3HT is in agreement with numerous reports [68]. The results suggest that isoindigo-copolymerization led to the formation of a J-aggregate, probably due to the extended conjugation length and planarization [98].

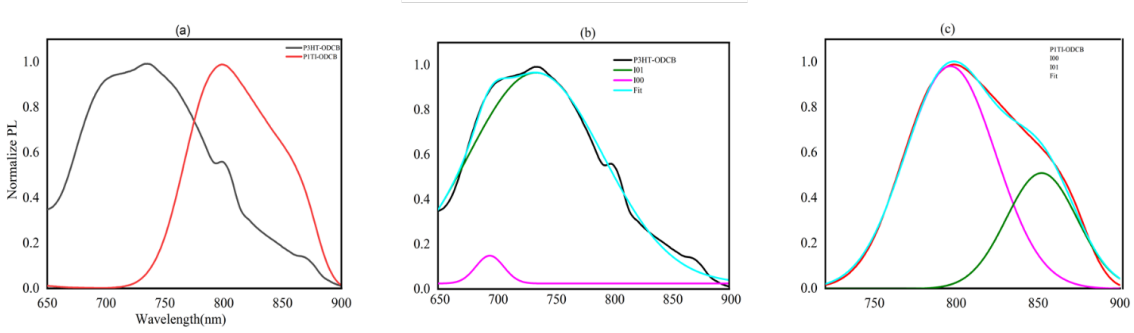

Figure 4.2: Photoluminescence (PL) spectra of P3HT and P1TI in o-DCB. (a) Comparison of normalized PL spectra for P3HT and P1TI, showing the red-shift of P1TI and blue-shift of P3HT, indicating J- and H-aggregation behavior, respectively. (b) Deconvolution of P3HT_o-DCB spectra into the 0-0 and 0-1 vibronic bands, with fitting curves. (c) Deconvolution of P1TI_o-DCB spectra into the 0-0 and 0-1 vibronic bands, showing a stronger contribution from the 0-0 transition, consistent with J-aggregation. The fitted curves are shown for comparison.

The aggregation type of the copolymers was further confirmed by comparing the intensity of the emission at the 0-0 and 0-1 transitions, as summarized in Table 4.4. In H-aggregates, the I_{00}/I_{01} ratio is 3.1, while in J-aggregates it is 0.27 [99]. The I_{00} is the dominant relaxation channel in P1TI, while it has a significantly lower emission in P3HT, confirming that P3HT and P1TI adopt H- and J-aggregates, respectively. The results were in agreement with the absorption measurements.

Table 4.4: Photoluminescence of P3HT and P1TI in o-DCB

Emissions	P3HT_o-DCB		P1TI_o-DCB	
	λ(nm)	Intensity	λ(nm)	Intensity
I_{00}	718.27	0.93	773.63	0.27
I_{01}	790.76	0.30	804.06	0.99
I_{00}/I_{01}	3.1		0.27	

4.3 Effect of Solvent on Aggregation Properties of P3HT and P1TI in CF and o-DCB

Aggregation of polymers is highly sensitive to the film formation process, including the solvent, spin casting speed, and concentration. In this regard, two solvents of different polarity and boiling points, o-DCB and CF, with polarity index (boiling point) of 2.7 and 4.2, respectively, were used to make the films. The absorption spectra of P3HT and P1TI are provided in Figure 4.3. The absorption of P3HT in CF was found to be blue-shifted with different vibronic features compared to the film prepared in o-DCB. On the contrary, the absorption of P1TI was red-shifted when CF was used, revealing a different spectral feature than the o-DCB film. At first glance, it can be seen that the aggregation of the two polymers changed due to the solvents used.

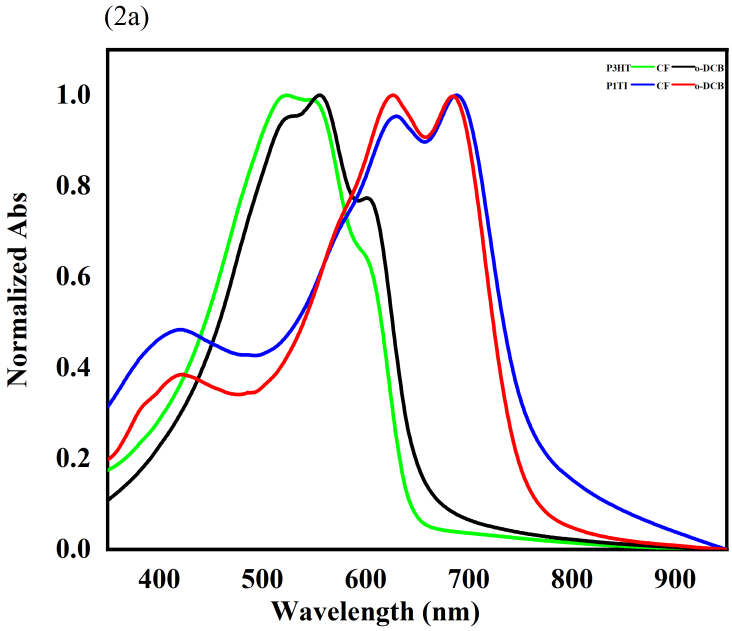

Figure 4.3: Normalized absorption spectra of P3HT and P1TI in different solvents: chlorobenzene (CF) and ortho-dichlorobenzene (o-DCB). The spectra display characteristic absorption peaks for both P3HT and P1TI, with distinct shifts observed between CF and o-DCB solutions. The green and black lines represent P3HT in CF and o-DCB, respectively, while the blue and red lines represent P1TI in CF and o-DCB, respectively. These spectral shifts are indicative of different molecular packing and aggregation behaviors influenced by the choice of solvent.

Hence, we further fitted the peaks of the polymers in the two solvents with Gaussian curves, as shown

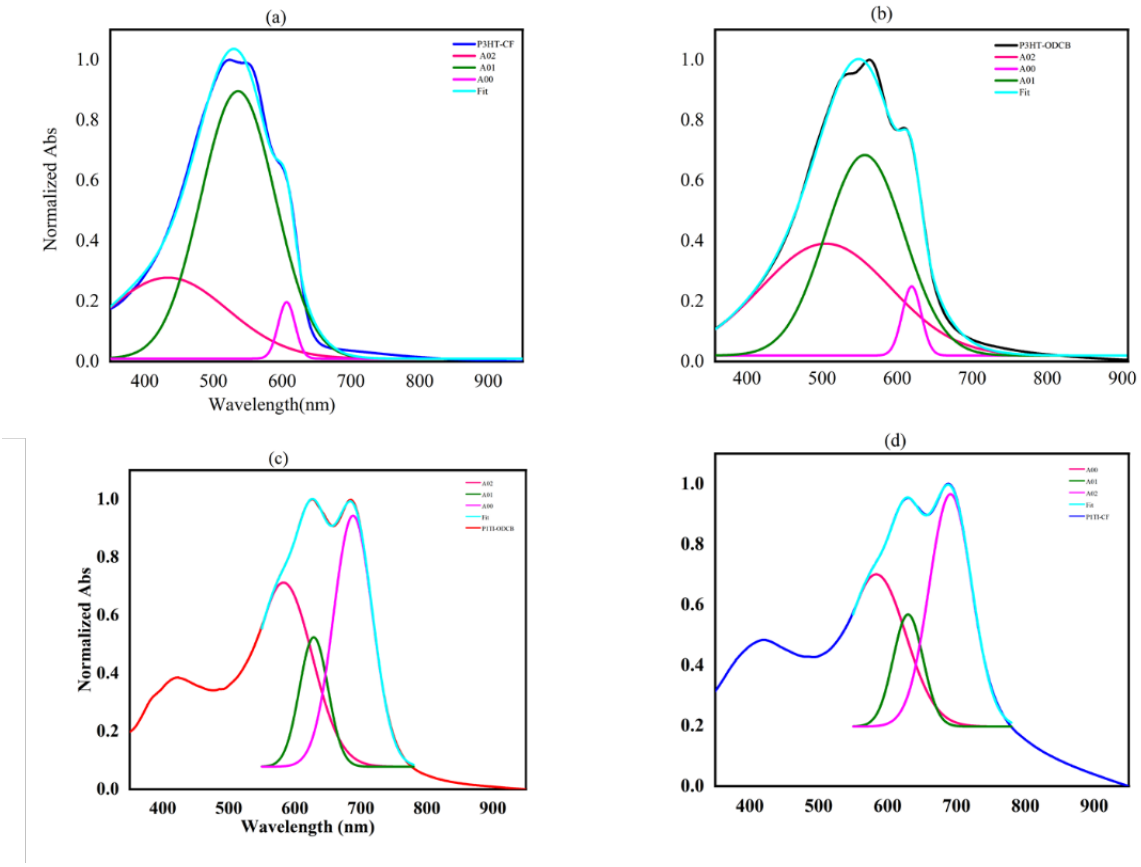

Figure 4.4: Normalized absorption spectra of P3HT and P1TI in different solvents and their deconvoluted vibronic bands. (a) P3HT in CF, showing a prominent A_{01} transition and fit curves indicating strong H-aggregation. (b) P3HT in o-DCB, with a higher A_{00}/A_{01} ratio suggesting weaker H-aggregation compared to CF. (c) P1TI in o-DCB, demonstrating a dominant A_{00} transition consistent with J-aggregation behavior. (d) P1TI in CF, with a mixed A_{00}/A_{01} transition indicating weaker H-aggregation compared to o-DCB. The fit curves for each spectrum reveal insights into the aggregation behaviors of the polymers based on the solvent.

in Figure 4.4. The A_{00} in P3HT decreased in CF compared to the o-DCB film, reducing the A_{00}/A_{01} ratio from 0.34 in o-DCB to 0.20 in CF. Similarly, the A_{00} transition was decreased in P1TI when CF was used as a solvent instead of o-DCB, decreasing the A_{00}/A_{01} from 1.79 (o-DCB) to 1.69 (CF). These results confirm that film aggregate formation could be tuned by the solvents used. It is known that CF is a low-boiling-point solvent that evaporates before full film formation during spin coating [100]. A number of reports on polymer solar cell active layers prepared using CF confirmed the formation of large aggregates [101]. Hence, it can also be seen in the films that the aggregate type of P3HT and P1TI is maintained to be H- and J-type, respectively. However, the strength of the H-aggregate in CF was higher, as the A_{00} transition was highly suppressed compared to the o-DCB. In contrast, the strength of J-aggregation in P1TI was lowered in CF, as seen by its lower A_{00}/A_{01} ratio. This could be due to the fact that the polymer might form large aggregates in the film in CF, which hampers the formation of tail-to-tail inter-chain interactions necessary to form J-aggregates. It therefore can be concluded low-boiling point solvents do not favour straight chain formation that could lead to J-aggregate formation

rather face-to-face packing is highly enhanced in the films due to the formation of large clusters in the films.

Table 4.5: Absorption of P3HT and P1TI in o-DCB & CF

Transition Band	**P3HT_CF**		**P3HT_o-DCB**		**P1TI_CF**		**P1TI_o-DCB**	
	λ in nm	**Abs.**	λ in nm	**Abs.**	λ in nm	**Abs.**	λ in nm	**Abs.**
A_{00}	606.55	0.18	611.85	0.24	691.36	0.95	688.20	0.93
A_{01}	535.87	0.88	549.26	0.69	629.75	0.56	628.64	0.52
A_{00}/A_{01}		0.20		0.34		1.69		1.78

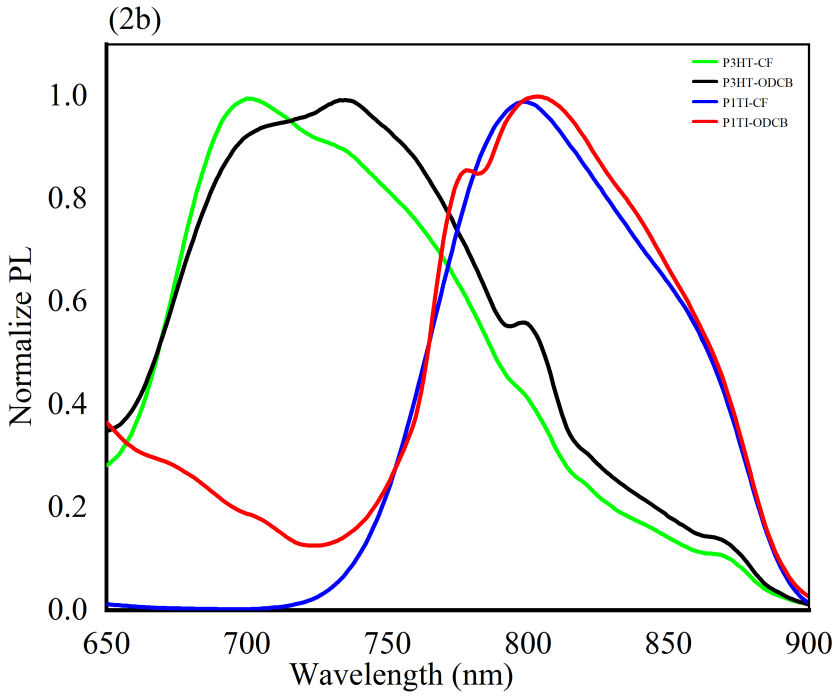

Figure 4.5: Normalized photoluminescence (PL) spectra of P3HT and P1TI in two solvents: chlorobenzene (CF) and ortho-dichlorobenzene (o-DCB). The green and black curves represent P3HT in CF and o-DCB, respectively, while the blue and red curves represent P1TI in CF and o-DCB, respectively. The shifts in the PL peaks reflect the impact of the solvent on molecular packing, with P1TI in o-DCB showing a significant red-shift and stronger emission, indicating J-aggregation, while P3HT shows H-aggregation behavior in both solvents.

The aggregation type of the copolymers was further confirmed by comparing the intensity of the emission at the 0-0 and 0-1 transitions, as summarized in Table 4.6. In P3HT_CF, the J-aggregate ratio of I_{00}/I_{01} is 0.38, while in P3HT_oDCB, the H-aggregate ratio is 3.1 [102]. The I_{00} is the dominant relaxation channel in P3HT_oDCB, while it has significantly lower emission in P3HT_CF, confirming that P3HT_oDCB and P3HT_CF adopt H- and J-aggregates, respectively. The H-aggregate ratio of I_{00}/I_{01} in P1TI_CF is 1.9, but the J-aggregate ratio in P1TI_oDCB is 0.27. P1TI_oDCB has a much lower emission in the I_{00} relaxation channel than P1TI_CF, indicating that P1TI_oDCB adopts a J-aggregate, while P1TI_CF adopts an H-aggregate [103]. The results were in agreement with the absorption measurements.

Table 4.6: Photoluminescence of P3HT and P1TI in o-DCB & CF

Emission	P3HT_CF		P3HT_o-DCB		P1TI_CF		P1TI_o-DCB	
	λ in nm	**Intensity**	λ in nm	**Intensity**	λ in nm	**Intensity**	λ in nm	**Intensity**
I_{00}	694.23	0.33	718.27	0.93	796.40	0.98	773.63	0.27
I_{01}	732.69	0.86	790.76	0.30	852.16	0.51	804.06	0.99
I_{00}/I_{01}		0.38		3.1		1.9		0.27

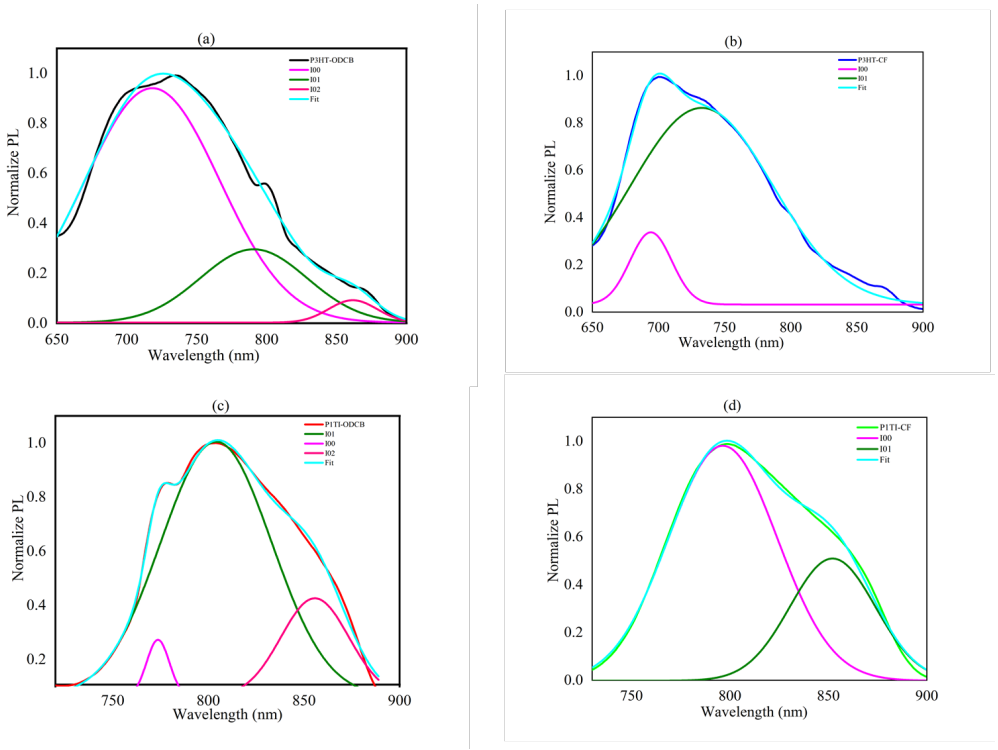

Figure 4.6: Gaussian fit of the photoluminescence (PL) spectra of P3HT and P1TI in different solvents, showing the decomposition of the spectra into individual vibronic transitions. (a) P3HT in o-DCB, with the fitting curves for the 0-0, 0-1, and 0-2 transitions, indicating H-aggregation. (b) P3HT in CF, showing a dominant 0-0 transition with relatively strong H-aggregation. (c) P1TI in o-DCB, demonstrating a dominant 0-0 transition, indicating strong J-aggregation behavior. (d) P1TI in CF, showing a more balanced contribution of the 0-0 and 0-1 transitions, indicating weaker J-aggregation compared to o-DCB. The Gaussian fits help to visualize the contributions of different vibronic bands to the overall PL spectra.

4.4 Effect of High Boiling Point Solvent Additives on Aggregation of P3HT and P1TI

In section 4.3, it was concluded that high boiling point solvents will be beneficial in providing the film enough time to avoid clusters. Here, we used a high boiling point additive, 1,8-diiodoocatne (DIO) to improve the films formation probably by reducing cluster formation. The Absorbance of P3HT and P1TI in CF and o-DCB with and without DIO is depicted in Figure 10. A slight red-shift was observed in both films when DIO was used. Additionally, a clear profile change in the vibronic features was observed, indicating the change in aggregate formation photophysics.

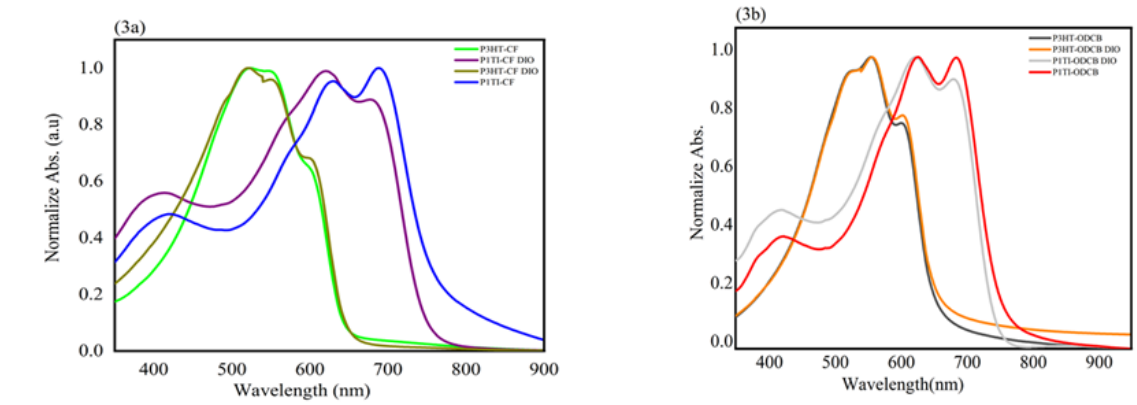

Figure 4.7: Normalized absorption spectra of P3HT and P1TI films in different solvent environments. (3a) Absorption spectra of P3HT_CF and P1TI_CF with and without DIO, showing changes in absorption characteristics. (3b) Absorption spectra of P3HT_ODCB and P1TI_ODCB with and without DIO, illustrating the effects of solvent and additive on the absorption profile.

-

Table 4.7: Absorption of P3HT and P1TI in CF & CF_DIO

Absorption	**P3HT_CF**		**P3HT_CF DIO**		**P1TI_CF**		**P1TI_CF DIO**	
	λ (nm)	**Abs.**	λ (nm)	**Abs.**	λ (nm)	**Abs.**	λ (nm)	**Abs.**
A_{00}	606.55	0.19	608.27	0.24	698.86	0.31	693.40	0.43
A_{01}	535.87	0.89	542.24	0.78	632.43	0.92	631.14	0.20
A_{00}/A_{01}		0.21		0.30		0.33		1.91

We therefore proceeded to the Gaussian fitting of the transition peak to easily allow us understand the aggregate types [104]. Figure 4.8 shows the fitting of the absorption spectra of P3HT and P1TI in CF with and without DIO. The corresponding fitting values are summarized in Table 4.7 The absorbance and photoluminescence characteristics of P3HT and P1TI can be greatly influenced by the addition of a high boiling point additive, such as DIO (1,8-diiodooctane), in a solvent solution (CF and o-DCB). The main cause of these modifications is that DIO has the power to change the solubility and crystallization behavior of polymers, which can change the way the chains of polymers cluster [105]. In $P3HT_{CF}$ and $P3HT_{CF\_DIO}$, this suggests that H-aggregation is indicated by the blue-shifted A_{00} transition. The presence of H-aggregation is supported by the very low A_{00}/A_{01} ratio (0.21 and 0.30) in both cases, where absorption in the lower-energy J-aggregate state (A_{01}) predominates over the blue-shifted A_{00} state. In $P1TI_{CF}$ with DIO, J-aggregation is indicated by a high A_{00}/A_{01} ratio of 1.91, while in $P1TI_{CF}$ without DIO, H-aggregation is generated by a low ratio of 0.33 [106].

Table 4.8: Absorption of P3HT and P1TI in o-DCB and o-DCB DIO

Absorption	**P3HT_o-DCB**		**P3HT_o-DCB DIO**		**P1TI_o-DCB**		**P1TI_o-DCB DIO**	
	λ (nm)	**Abs.**	λ (nm)	**Abs.**	λ (nm)	**Abs.**	λ (nm)	**Abs.**
A_{00}	611.74	0.23	612.52	0.29	692.78	0.52	690.83	0.59
A_{01}	548.50	0.66	552.69	0.61	628.08	0.21	630.46	0.26
A_{00}/A_{01}		0.34		0.47		2.5		2.26

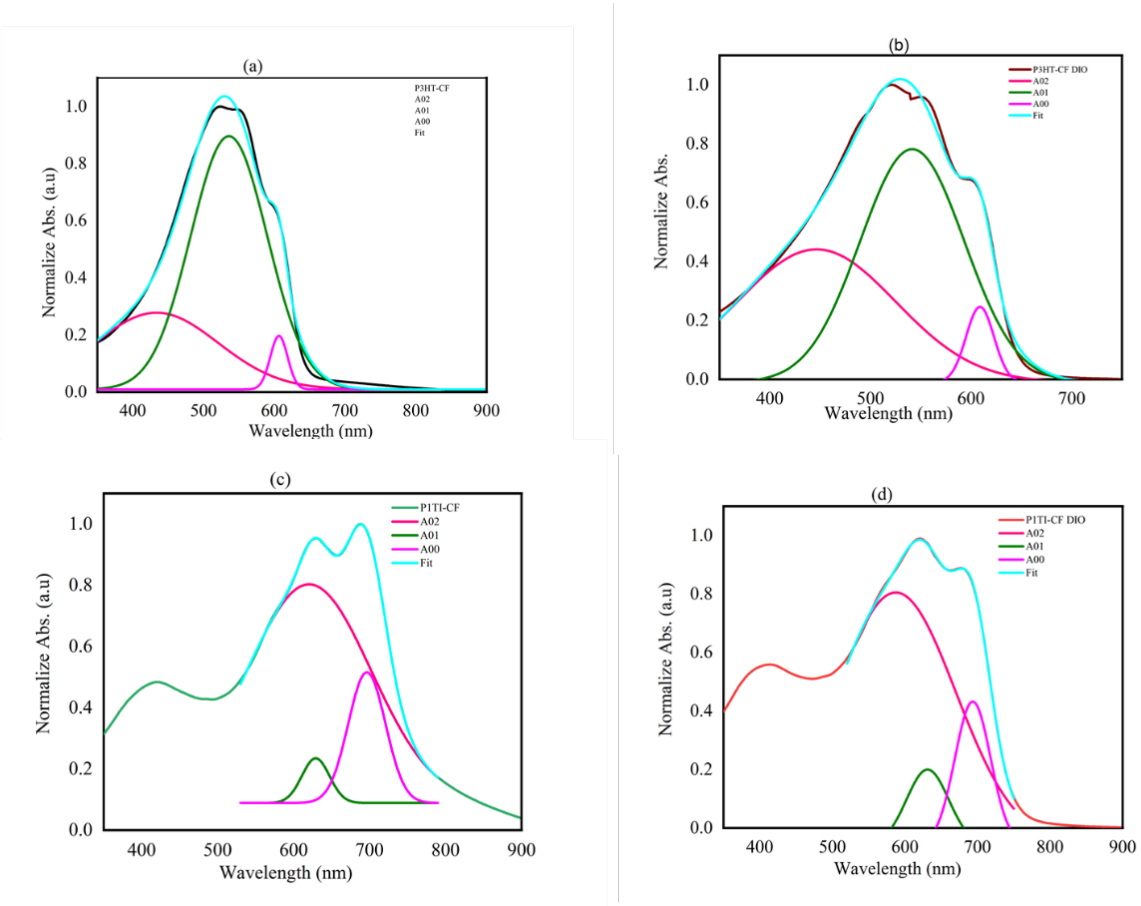

Figure 4.8: Gaussian fit of the absorbance spectra of P3HT and P1TI in chlorobenzene (CF) with and without the high boiling point additive diiodooctane (DIO). (a) P3HT in CF without DIO shows characteristic peaks corresponding to the vibronic transitions A_{00}, A_{01}, and A_{02}. (b) P3HT in CF with DIO exhibits a red shift and an increased intensity of A_{00}, indicating enhanced J-aggregation. (c) P1TI in CF without DIO displays prominent peaks corresponding to vibronic transitions, highlighting strong H-aggregation. (d) P1TI in CF with DIO shows a significant red shift and increased A_{00}, suggesting a shift toward J-aggregation.

As shown in Figure 4.9, the absorption spectra with ODCB as the solvent show a different pattern compared to the CF solvent. The use of ODCB leads to a more significant red shift in the absorption maxima, with the peaks appearing at longer wavelengths for both P3HT_ODCB and P1TI_ODCB. The addition of DIO again increases the absorbance intensity, particularly for P1TI_ODCB [107]. As can be seen from the analysis on the Gaussian Fit (Table 4.10, for P3HT_ODCB without DIO, the peaks are observed at 611.74 nm (A_{00}) and 548.50 nm (A_{01}), with a ratio of A_{00}/A_{01}=0.34, indicating more balanced absorption compared to the CF case. With DIO, the peaks shift slightly to 612.52 nm and 552.69 nm, with a higher absorbance ratio of 0.47, indicating enhanced absorption efficiency due to improved film morphology with DIO. For P1TI_ODCB without DIO, the peaks occur at 692.78 nm and 628.08 nm, with a high absorbance ratio A_{00}/A_{01}=2.5. This suggests that the low-energy absorption is much more pronounced, likely due to increased molecular ordering. When DIO is added, the peaks shift slightly to 690.83 nm and 630.46 nm, and the absorbance ratio is slightly reduced to 2.26, suggesting a similar but slightly

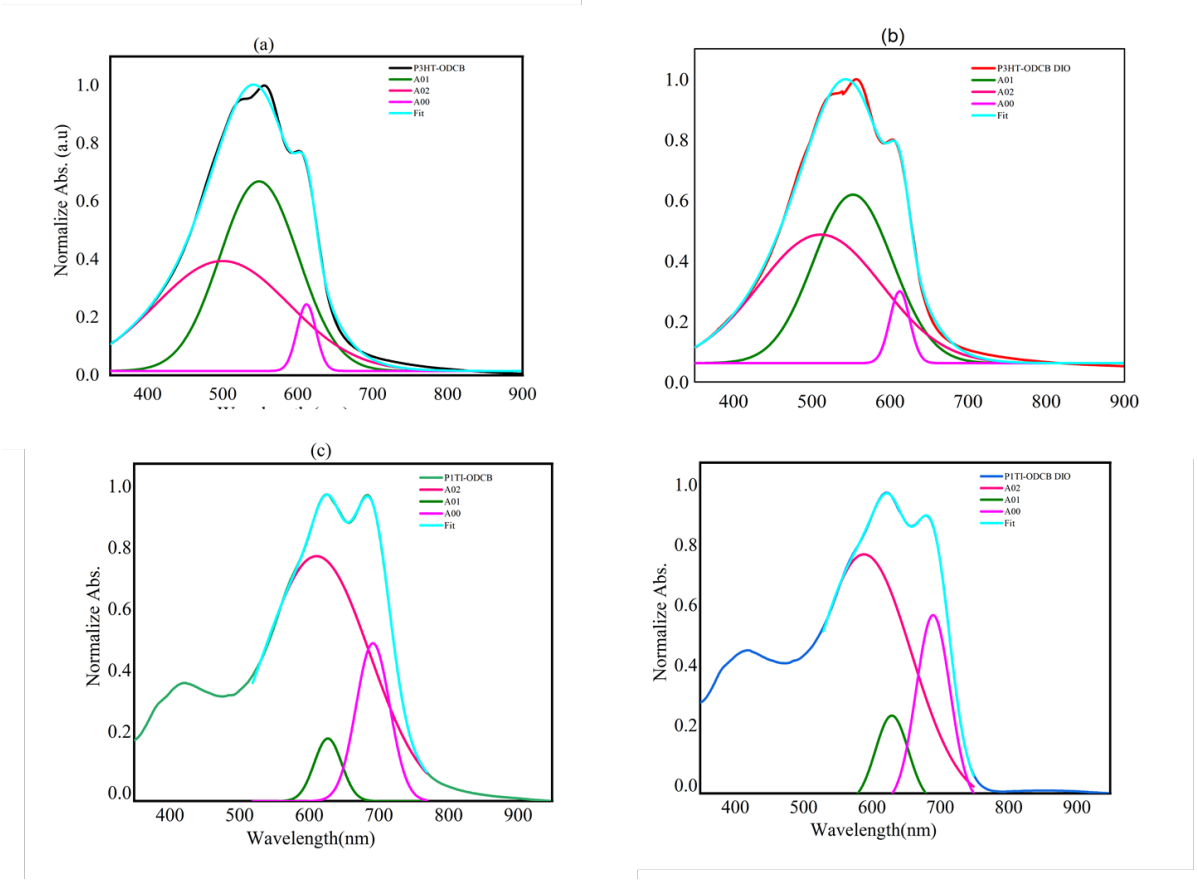

Figure 4.9: Gaussian fit of the absorbance spectra of P3HT and P1TI in o-DCB with and without di-iodooctane (DIO). (a) P3HT in o-DCB without DIO shows the vibronic transitions A_{00}, A_{01}, and A_{02}, indicating strong H-aggregation behavior. (b) P3HT in o-DCB with DIO shows a red-shift in A_{00} and A_{01}, indicating enhanced J-aggregation. (c) P1TI in o-DCB without DIO exhibits typical transitions associated with H-aggregation, with A_{00} dominating. (d) P1TI in o-DCB with DIO shows a red-shift in the A_{00} and A_{01} peaks, suggesting a shift toward J-aggregation, similar to P3HT.

less efficient absorption structure compared to the case without DIO.

The photoluminescence (PL) spectra presented in Figures 4.10, along with the Gaussian fit data from Tables 4.9 and 4.10, provide insight into how the polymer chain interactions, solvents, and additives (DIO and ODCB) affect the emissive properties of P3HT and P1TI films.

As shown in Figure 4.10-left and Table 4.9 (P3HT_CF and P1TI_CF with/without DIO), the normalized PL spectra of P3HT_CF and P1TI_CF show red-shifted and enhanced emission in the presence of DIO, suggesting improved molecular ordering. However, based on the I_{00}/I_{01} ratio, for P3HT_CF without DIO, the ratio is 0.38, which is less than 1, indicating J-aggregate behavior. With DIO, the ratio increases to 0.79, which still indicates J-aggregation, but the higher value suggests reduced exciton coupling compared to the non-DIO case, which might indicate some H-aggregate influence starting to appear but still dominated by J-aggregates. On the other hand, for P1TI_CF, the situation is different. The I_{00}/I_{01} ratio

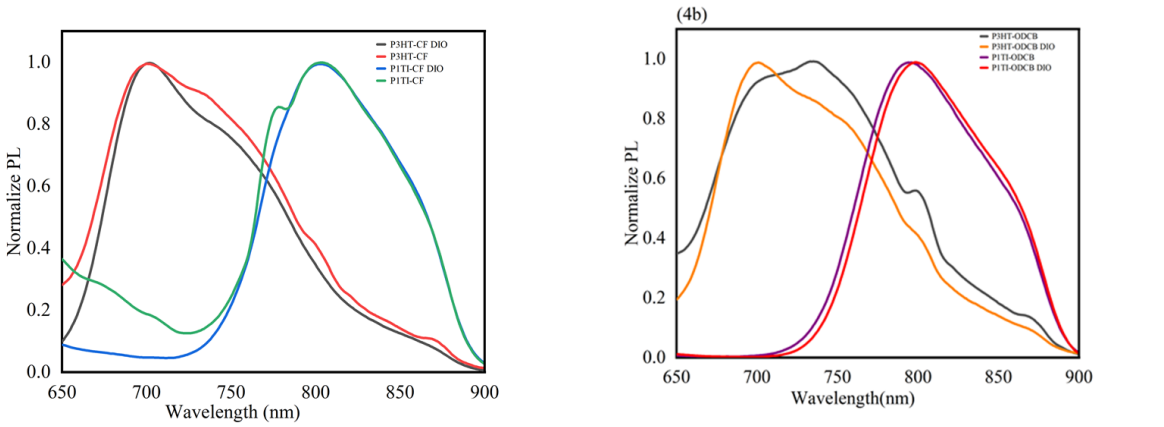

Figure 4.10: Photoluminescence (PL) spectra of P3HT and P1TI films in different solvent environments. *Left:* PL spectra of P3HT_CF and P1TI_CF with/without DIO, showing the effect of molecular ordering and J-aggregation behavior. *Right:* PL spectra of P3HT_ODCB and P1TI_ODCB with/without DIO, indicating a transition from H-aggregation to J-aggregation in P3HT_ODCB upon the addition of DIO, while P1TI_ODCB maintains strong H-aggregation characteristics.

is 1.9 without DIO, which suggests H-aggregate behavior is dominant. Adding DIO reduces the ratio to 1.61, meaning that while H-aggregates still dominate, DIO slightly weakens their influence, possibly introducing some molecular reorganization that favors J-aggregation.

Similarly, as shown in Figure 4.10-right and Table 4.10 (P3HT_ODCB and P1TI_ODCB with/without DIO), in ODCB, P3HT_ODCB shows a red shift in the spectra, indicating improved molecular packing. As can visually seen in the Guassian fit Figure 4.12 and according to the I_{00}/I_{01} ratio result for P3HT_ODCB without DIO is 3.1, which strongly suggests H-aggregate behavior. The addition of DIO lowers this ratio to 0.52, showing a transition to J-aggregate behavior. This implies that DIO disrupts the H-aggregates and induces a more favorable J-aggregate structure for light emission in P3HT_ODCB. However, for P1TI_ODCB, the ratio is 2.5 without DIO and 2.26 with DIO, both indicating strong H-aggregation. The small decrease in the ratio with DIO suggests a minor disruption of the H-aggregate structure but does not lead to a transition to J-aggregation. Therefore, our results align with the established understanding that $I_{00}/I_{01} > 1$ corresponds to H-aggregate behavior and $I_{00}/I_{01} < 1$ indicates J-aggregates. In both CF and ODCB solvents, the introduction of DIO generally reduces the dominance of H-aggregates, promoting J-aggregate formation, particularly in P3HT_ODCB. However, in cases like P1TI_CF and P1TI_ODCB, the materials exhibit dominant H-aggregation behavior, even with DIO, which enhances packing but does not fully transition to J-aggregation.

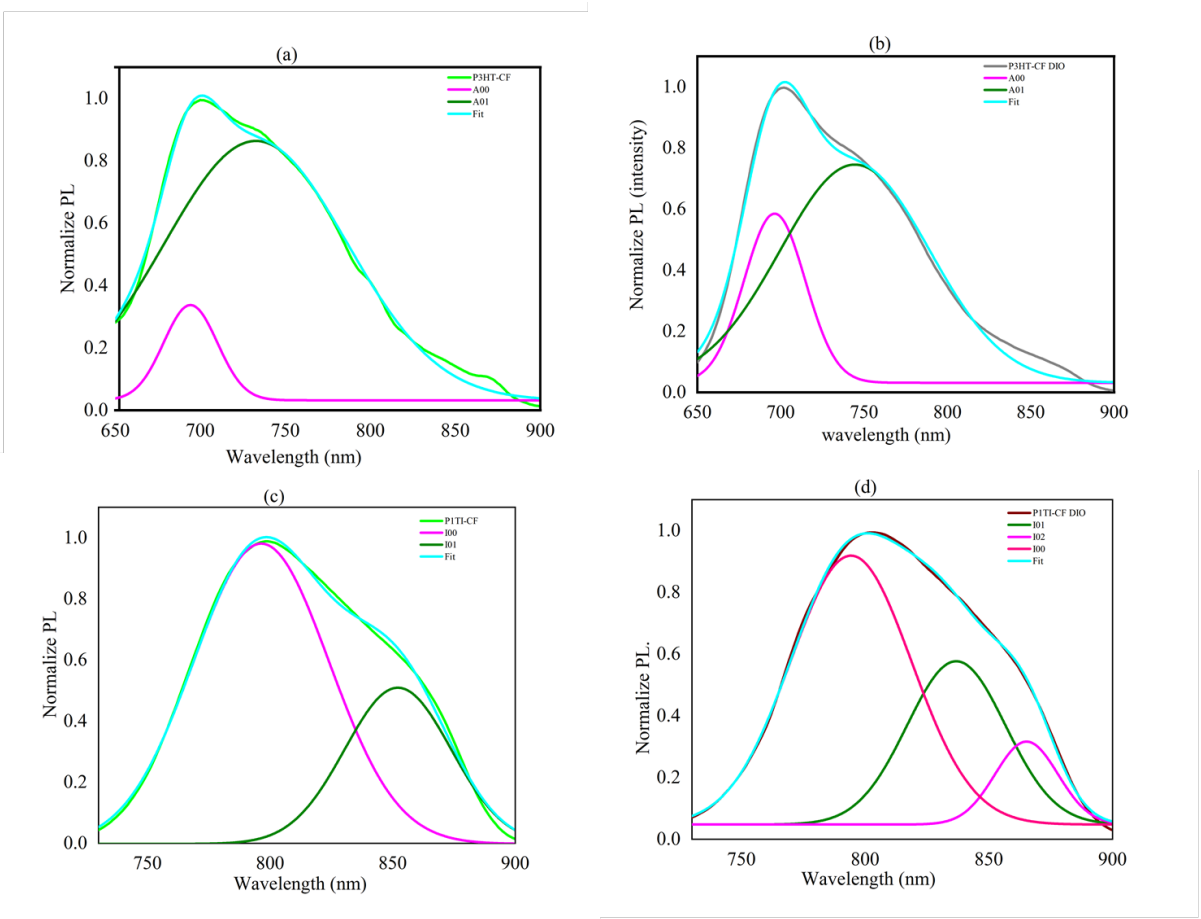

Figure 4.11: Photoluminescence (PL) spectra of P3HT and P1TI films in CF solvent with and without DIO. (a) PL spectra of P3HT_CF without DIO, showing the contributions of A_{00}, A_{01} components, and the overall fit. (b) PL spectra of P3HT_CF with DIO, illustrating changes in the emission components and the fit. (c) PL spectra of P1TI_CF without DIO, showing the contributions of I_{00}, I_{01} components and the overall fit. (d) PL spectra of P1TI_CF with DIO, indicating the changes in emission behavior with the addition of DIO.

Table 4.9: The result of Gaussian Fit of PL of a) P3HT_CF without DIO b) P3HT_CF with DIO c) P1TI_CF without DIO d) P1TI_CF with DIO

Emission	**P3HT_CF with DIO**		**P3HT_CF w/out DIO**		**P1TI_CF with DIO**		**P1TI_CF w/out DIO**	
	λ (nm)	**Intensity**	λ (nm)	**Intensity**	λ (nm)	**Intensity**	λ (nm)	**Intensity**
I_{00}	696.35	0.59	694.23	0.33	794.29	0.92	796.40	0.98
I_{01}	744.48	0.74	732.69	0.86	836.85	0.57	852.16	0.51
I_{00}/I_{01}	0.79		0.38		1.61		1.9	

Table 4.10: The result of Gaussian Fit of PL of a) P3HT_ODCB with out DIO b) P3HT_ODCB with DIO c) P1TI_ODCB with out DIO d) P1TI_ODCB with DIO

Emission	**P3HT_ODCB with DIO**		**P3HT_ODCB w/out DIO**		**P1TI_ODCB with DIO**		**P1TI_ODCB w/out DIO**	
	λ (nm)	**Intensity**	λ (nm)	**Intensity**	λ (nm)	**Intensity**	λ (nm)	**Intensity**
I_{00}	718.27	0.93	694.59	0.43	773.63	0.27	796.40	0.98
I_{01}	790.76	0.30	738.72	0.82	804.06	0.99	852.16	0.51
I_{00}/I_{01}	3.1		0.52		0.27		1.9	

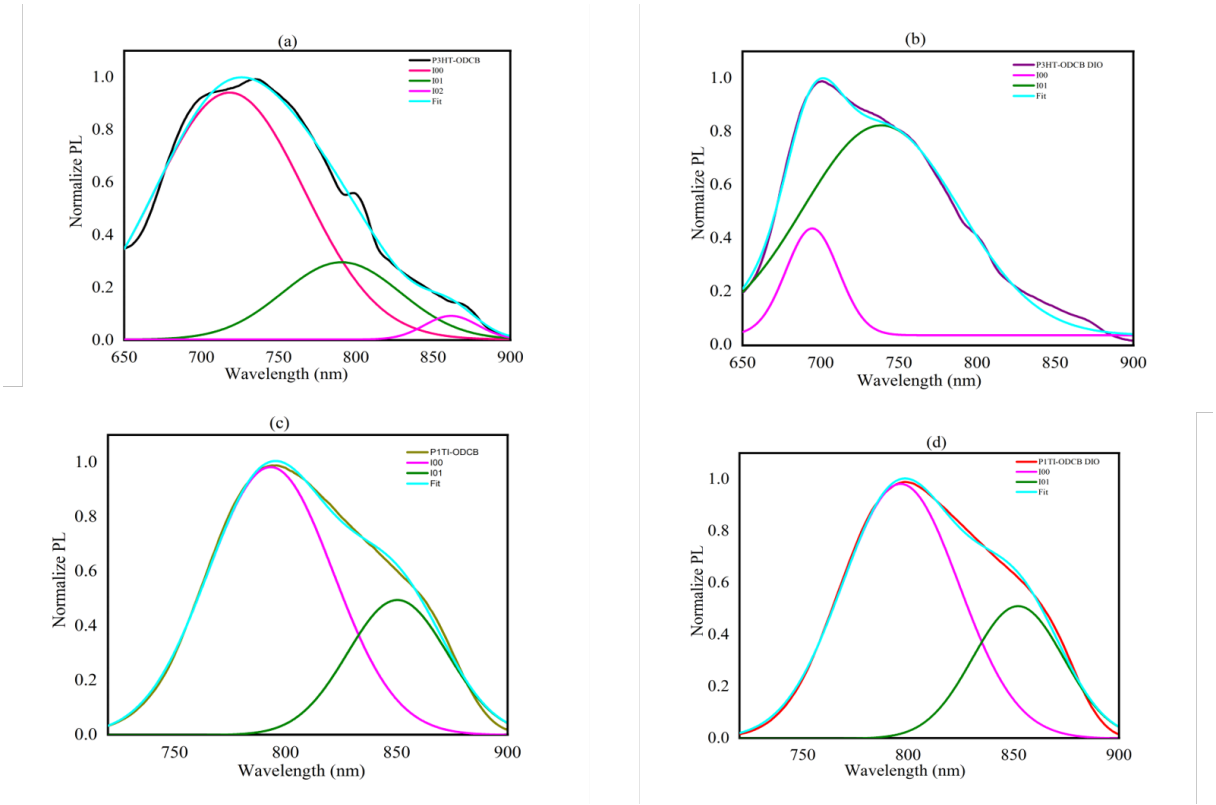

Figure 4.12: Photoluminescence (PL) spectra of P3HT and P1TI films with ODCB as the solvent, with-/without DIO. (a) PL spectra of P3HT_ODCB without DIO showing the contributions of different emission components (I_{00}, I_{01}, I_{02}) and the fit. (b) PL spectra of P3HT_ODCB with DIO, illustrating the changes in emission components and the fit. (c) PL spectra of P1TI_ODCB without DIO showing the contributions of I_{00}, I_{01} components and the fit. (d) PL spectra of P1TI_ODCB with DIO, highlighting the effects of DIO on emission and the overall fit.

Chapter 5

CONCLUSION AND RECOMMENDATION

5.1 Conclusion

This study explores the optical properties of P3HT and P1TI under varied conditions including different solvents, the presence of high boiling point additives, and annealing. Insights from this research highlight how these polymers aggregate, significantly impacting their performance in optoelectronic applications such as organic light-emitting diodes (OLEDs) and organic photovoltaics (OPVs).

The choice of solvent (o-DCB vs. CF) greatly influences the aggregation behavior of P3HT and P1TI. In o-DCB, both polymers exhibit more pronounced H-aggregation (indicated by higher A_{00}/A_{01} and I_{00}/I_{01} ratios), suggesting enhanced chain ordering and greater exciton delocalization. Conversely, CF promotes stronger J-aggregation in P1TI, and enhanced H-aggregation in both polymers, leading to more localized exciton states beneficial for certain device applications.

The incorporation of high boiling point additives such as DIO significantly modifies the aggregation characteristics, encouraging J-aggregation in both P3HT and P1TI. This is evidenced by increased A_{00}/A_{01} and I_{00}/I_{01} ratios in absorption and photoluminescence spectra. The reduction in H-aggregation due to DIO leads to improved exciton mobility and enhanced charge transport, which are critical for the efficiency of organic solar cells.

P3HT consistently shows a larger Stokes shift compared to P1TI, suggesting more disordered excited states in P3HT. In contrast, the smaller Stokes shift in P1TI implies a higher degree of crystallinity, which

could be advantageous in applications requiring reduced reorganization energy during excitation.

5.2 Recommendations

For applications requiring J-aggregation and superior chain ordering, such as in organic photovoltaics, o-DCB should be the preferred solvent for both P3HT and P1TI. Conversely, CF is recommended when H-aggregation is beneficial, such as in thin-film transistors where compact packing and localized excitons can enhance charge transfer efficiency.

The use of high boiling point additives like DIO is recommended to further promote J-aggregation and improve exciton mobility and charge separation key processes for enhancing the efficiency of organic solar cells.Post-fabrication annealing should be adopted as a standard practice to improve molecular ordering and crystallinity, particularly where J-aggregation is beneficial. The annealing conditions, including temperature and duration, should be specifically tailored to the polymer-solvent system. For instance, while annealing in o-DCB may significantly enhance the properties of P1TI, it could increase H-aggregation in P3HT, necessitating careful control of the annealing process.

Bibliography

[1] Baocai Du et al. “Heating induced aggregation in non-fullerene organic solar cells towards high performance”. In: *Journal of Energy Chemistry* 54 (2021), pp. 131–137.

[2] Qishi Liu et al. “18% Efficiency organic solar cells”. In: *Science Bulletin* 65.4 (2020), pp. 272–275.

[3] Ebru Kondolot Solak and Erdal Irmak. “Advances in organic photovoltaic cells: A comprehensive review of materials, technologies, and performance”. In: *RSC advances* 13.18 (2023), pp. 12244–12269.

[4] Yong Cui et al. “Single-junction organic photovoltaic cells with approaching 18% efficiency”. In: *Advanced Materials* 32.19 (2020), p. 1908205.

[5] Holger Spanggaard and Frederik C Krebs. “A brief history of the development of organic and polymeric photovoltaics”. In: *Solar Energy Materials and Solar Cells* 83.2-3 (2004), pp. 125–146.

[6] Md Meganur Rhaman and MA Matin. “Organic Solar Cells: Historical developments and challenges”. In: *2015 International Conference on Advances in Electrical Engineering (ICAEE)*. IEEE. 2015, pp. 26–29.

[7] Markus Clark Scharber and Niyazi Serdar Sariciftci. “Efficiency of bulk-heterojunction organic solar cells”. In: *Progress in polymer science* 38.12 (2013), pp. 1929–1940.

[8] Steffen Roland. “Charge carrier recombination and open circuit voltage in organic solar cells: from bilayer-model systems to hybrid multi-junctions”. PhD thesis. Universität Potsdam, 2017.

[9] Ebru Kondolot Solak and Erdal Irmak. “6. Advances in organic photovoltaic cells: a comprehensive review of materials, technologies, and performance”. In: *RSC Advances* (2023).

[10] Yen-Ju Cheng, Sheng-Hsiung Yang, and Chain-Shu Hsu. “Synthesis of conjugated polymers for organic solar cell applications”. In: *Chemical reviews* 109.11 (2009), pp. 5868–5923.

[11] Mantas Jakučionis, Agnius Žukas, and Darius Abramavicius. “5. Modeling molecular J and H aggregates using multiple-Davydov D2 ansatz.” In: *Physical Chemistry Chemical Physics* (2022).

[12] Jin-Bo Zhu et al. “2. Impact of backbone linkage positions on the molecular aggregation behavior of polymer photovoltaic materials.” In: *Physical Chemistry Chemical Physics* (2022).

[13] Ahmed G.S. Al-Azzawi et al. “9. A Mini Review on the Development of Conjugated Polymers: Steps towards the Commercialization of Organic Solar Cells”. In: *Polymers* (2022).

[14] Jiajun Xu et al. “1. CH··· interaction induced H-aggregates for wide range water content detection in organic solvents”. In: *Aggregate* (2024).

[15] Xin Chang, Mohammad Balooch Qarai, and Frank C. Spano. “3. Intermolecular Charge Transfer in H- and J-Aggregates of Donor–Acceptor–Donor Chromophores: The Curious Case of Bithiophene-DPP”. In: *Journal of Physical Chemistry C* (2022).

[16] Pen-Cheng Wang et al. “Transparent electrodes based on conducting polymers for display applications”. In: *Displays* 34.4 (2013), pp. 301–314.

[17] Eninges Asmare et al. “Conformation-Dictated Aggregation Photophysics in Isoindigo-Based Copolymers”. In: *The Journal of Physical Chemistry C* (2024).

[18] Bo Liu et al. “Low bandgap isoindigo-based copolymers: design, synthesis and photovoltaic applications”. In: *Polymer Chemistry* 2.5 (2011), pp. 1156–1162.

[19] Mingliang Zhu, Yunlong Guo, and Yunqi Liu. “A thriving decade: rational design, green synthesis, and cutting-edge applications of isoindigo-based conjugated polymers in organic field-effect transistors”. In: *Science China Chemistry* 65.7 (2022), pp. 1225–1264.

[20] Bao Zhang et al. “The first application of isoindigo-based polymers in non-fullerene organic solar cells”. In: *Science China Chemistry* 63 (2020), pp. 1262–1271.

[21] Hansol Lee et al. “Effect of donor–acceptor molecular orientation on charge photogeneration in organic solar cells”. In: *NPG Asia Materials* 10.6 (2018), pp. 469–481.

[22] Fei Dou et al. “Controlling molecule aggregation and electronic spatial coherence in the h-aggregate and j-aggregate regime at room temperature”. In: *Polymers* 12.4 (2020), p. 786.

[23] Frank C Spano and Carlos Silva. “H-and J-aggregate behavior in polymeric semiconductors”. In: *Annual review of physical chemistry* 65.1 (2014), pp. 477–500.

[24] Dong Hwan Wang et al. “Enhanced high-temperature long-term stability of polymer solar cells with a thermally stable TiO x interlayer”. In: *The Journal of Physical Chemistry C* 113.39 (2009), pp. 17268–17273.

[25] Jang-Joo Kim, Min-Koo Han, and Yong-Young Noh. “Flexible OLEDs and organic electronics”. In: *Semiconductor Science and Technology* 26.3 (2011), p. 030301.

[26] Marco Stella. *Study of organic semiconductors for device applications*. Universitat de Barcelona, 2010.

[27] Xinzhao Xu, Yan Zhao, and Yunqi Liu. “Wearable electronics based on stretchable organic semiconductors”. In: *Small* 19.20 (2023), p. 2206309.

[28] Yingxin Ma et al. “2D optical waveguides based on hierarchical organic semiconductor single crystals”. In: *Advanced Optical Materials* 9.22 (2021), p. 2101481.

[29] Yuanhe Wang et al. “Flexible organic optoelectronic devices: Design, fabrication, and applications”. In: *APL Photonics* 9.9 (2024).

[30] Dominik Landerer et al. “Solar Glasses: A Case Study on Semitransparent Organic Solar Cells for Self-Powered, Smart, Wearable Devices”. In: *Energy Technology* 5.11 (2017), pp. 1936–1945.

[31] Frederick T Wall. “The Structure of Copolymers. II1”. In: *Journal of the American Chemical Society* 66.12 (1944), pp. 2050–2057.

[32] Seth B Darling. “Block copolymers for photovoltaics”. In: *Energy & Environmental Science* 2.12 (2009), pp. 1266–1273.

[33] Prashant Sonar et al. “Isoindigo dye incorporated copolymers with naphthalene and anthracene: Promising materials for stable organic field effect transistors”. In: *Polymer Chemistry* 4.6 (2013), pp. 1983–1994.

[34] Chun-Chih Ho et al. “Isoindigo-based copolymers for polymer solar cells with efficiency over 7%”. In: *Journal of Materials Chemistry A* 2.21 (2014), pp. 8026–8032.

[35] Kazuhiro Nakabayashi, Kosei Miyakawa, and Hideharu Mori. “Thienoisoindigo-based donor-acceptor random copolymers: synthesis, characterization, and thin film nanostructure study”. In: *Polymer Bulletin* 77.8 (2020), pp. 4011–4022.

[36] Yu-Ting Liao et al. “Solution-processed isoindigo-and thienoisoindigo-based donor–acceptor–donor π-conjugated small molecules: synthesis, morphology, molecular packing, and field-effect transistor characterization”. In: *ACS Applied Materials & Interfaces* 14.50 (2022), pp. 55886–55897.

[37] Arelis Ledesma-Juárez et al. “Structure modification of isoindigo copolymer synthesized by direct arylation that improves the open circuit voltage on organic solar cells”. In: *Journal of Molecular Structure* 1275 (2023), p. 134636.

[38] Bao Zhang et al. “The first application of isoindigo-based polymers in non-fullerene organic solar cells”. In: *Science China Chemistry* (2020), pp. 1–10. URL: https://api.semanticscholar.org/CorpusID:220324406.

[39] Raymond N. Bennett et al. “Bisisoindigo–Benzothiadiazole Copolymers: Materials for Ambipolar and n-Channel OTFTs with Low Threshold Voltages”. In: *ACS Applied Electronic Materials* (2020). URL: https://api.semanticscholar.org/CorpusID:219910707.

[40] Qian Liu et al. “Triethylene Glycol Substituted Diketopyrrolopyrrole- and Isoindigo-Dye Based Donor–Acceptor Copolymers for Organic Light-Emitting Electrochemical Cells and Transistors”. In: *Advanced Electronic Materials* 6 (2020). URL: https://api.semanticscholar.org/CorpusID:216185636.

[41] Chanwoo Kim et al. “Aggregates of conjugated polymers: bottom-up control of mesoscopic morphology and photophysics”. In: *NPG Asia Materials* 15 (2023), pp. 1–13. URL: https://api.semanticscholar.org/CorpusID:258766405.

[42] Qingyun Wan and Chi-Ming Che. “Role of Centrosymmetry in the Photophysics of Molecular Aggregates”. In: 2023. URL: https://api.semanticscholar.org/CorpusID:263830852.

[43] Sergey Usoltsev et al. “Variety of steady and excited state interactions in BODIPY aggregates: photophysics in antisolvent systems and floating layers”. In: *Journal of Molecular Liquids* (2023). URL: https://api.semanticscholar.org/CorpusID:256680924.

[44] Pouria Ramezani, Stefaan C De Smedt, and Félix Sauvage. “Supramolecular dye nanoassemblies for advanced diagnostics and therapies”. In: *Bioengineering & Translational Medicine* (2024), e10652.

[45] Michael Kasha. “Characterization of electronic transitions in complex molecules”. In: *Discussions of The Faraday Society* 9 (1950), pp. 14–19. URL: https://api.semanticscholar.org/CorpusID:98501151.

[46] Suiying Ye et al. “Strong Aggregate Emission of Perylene Diimide in Solid State Enabled by Polymerization-Mediated Charge Transfer”. In: (2023).

[47] Eion G. McRae and Michael Kasha. “Enhancement of Phosphorescence Ability upon Aggregation of Dye Molecules”. In: *Journal of Chemical Physics* 28 (1958), pp. 721–722. URL: https://api.semanticscholar.org/CorpusID:96671782.

[48] Quinn Burlingame et al. “5. Voltage-dependent excitation dynamics in UV-absorbing organic photovoltaics with efficient charge transfer exciton emission”. In: *Energy and Environmental Science* (2022).

[49] Yong-Yu Xu. “3. Bridging the gap between H- and J-aggregates: Classification and supramolecular tunability for excitonic band structures in two-dimensional molecular aggregates”. In: *Chemical physics reviews* (2022).

[50] Sumit Kumar Patra, Ramalingam Manivannan, and Young-A Son. “5. Multicolor emissive organic material to display aggregation caused red shift with dual state emission, and application towards rewritable data storage”. In: *Journal of Photochemistry and Photobiology A-chemistry* (2023).

[51] David Beljonne et al. “Interchain vs. intrachain energy transfer in acceptor-capped conjugated polymers”. In: *Proceedings of the National Academy of Sciences of the United States of America* 99 (2002), pp. 10982–10987. URL: https://api.semanticscholar.org/CorpusID:31883363.

[52] Ary R Murad et al. “Conducting Polymers for Optoelectronic Devices and Organic Solar Cells: A Review”. In: *Polymers* 12 (2020). URL: https://api.semanticscholar.org/CorpusID:226853562.

[53] Wenjing Hou et al. “The Applications of Polymers in Solar Cells: A Review”. In: *Polymers* 11 (2019). URL: https://api.semanticscholar.org/CorpusID:91185985.

[54] Mohamad S. Alsalhi et al. “Recent Advances in Conjugated Polymers for Light Emitting Devices”. In: *International Journal of Molecular Sciences* 12 (2011), pp. 2036–2054. URL: https://api.semanticscholar.org/CorpusID:24603295.

[55] Namsheer K. and Chandra Sekhar Rout. “Conducting polymers: a comprehensive review on recent advances in synthesis, properties and applications”. In: *RSC Advances* 11 (2021), pp. 5659–5697. URL: https://api.semanticscholar.org/CorpusID:234075643.

[56] Felipe A. Angel, María Belén Camarada, and Ignacio A. Jessop. “Computational chemistry advances on benzodithiophene-based organic photovoltaic materials”. In: *Critical Reviews in Solid State and Materials Sciences* 48 (2022), pp. 333–360. URL: https://api.semanticscholar.org/CorpusID:247835383.

[57] Kerui Liu et al. “Organic Solar Cells with Over 19% Efficiency Enabled by a 2D-Conjugated Non-Fullerene Acceptor Featuring Favorable Electronic and Aggregation Structures”. In: *Advanced Materials* 35 (2023). URL: https://api.semanticscholar.org/CorpusID:258948476.

[58] Rui Sun et al. “Single-Junction Organic Solar Cells with 19.17% Efficiency Enabled by Introducing One Asymmetric Guest Acceptor”. In: *Advanced Materials* 34 (2022). URL: https://api.semanticscholar.org/CorpusID:248242142.

[59] Xiangzhi Li et al. “Effect of fluorination on n-type conjugated polymers for all-polymer solar cells”. In: *RSC Advances* 7 (2017), pp. 17076–17084. URL: https://api.semanticscholar.org/CorpusID:99285449.

[60] Henning Sirringhaus et al. “Two-dimensional charge transport in self-organized, high-mobility conjugated polymers”. In: *Nature* 401 (1999), pp. 685–688. URL: https://api.semanticscholar.org/CorpusID:4387286.

[61] Richard D Mccullough et al. “Self-orienting head-to-tail poly(3-alkylthiophenes): new insights on structure-property relationships in conducting polymers”. In: *Journal of the American Chemical Society* 115 (1993), pp. 4910–4911. URL: https://api.semanticscholar.org/CorpusID:15848137.

[62] R. Joseph Kline and Michael D. McGehee. “Morphology and Charge Transport in Conjugated Polymers”. In: *Journal of Macromolecular Science, Part C* 46 (2006), pp. 27–45. URL: https://api.semanticscholar.org/CorpusID:18205785.

[63] Frank C. Spano. “Modeling disorder in polymer aggregates: the optical spectroscopy of regioregular poly(3-hexylthiophene) thin films.” In: *The Journal of chemical physics* 122 23 (2005), p. 234701. URL: https://api.semanticscholar.org/CorpusID:32984229.

[64] Jenny Clark et al. “Role of intermolecular coupling in the photophysics of disordered organic semiconductors: aggregate emission in regioregular polythiophene.” In: *Physical review letters* 98 20 (2007), p. 206406. URL: https://api.semanticscholar.org/CorpusID:12684913.

[65] Adam J. Moulé and Klaus Meerholz. “Controlling Morphology in Polymer–Fullerene Mixtures”. In: *Advanced Materials* 20 (2008). URL: https://api.semanticscholar.org/CorpusID:137313225.

[66] Solenn Berson et al. “Poly(3-hexylthiophene) Fibers for Photovoltaic Applications”. In: *Advanced Functional Materials* 17 (2007). URL: https://api.semanticscholar.org/CorpusID:96403524.

[67] Leyi Tang et al. “Fluorine substitution for aggregation transformation and exciton dissociation acceleration in non-fused electron acceptors”. In: *Chemical Engineering Journal* (2024). URL: https://api.semanticscholar.org/CorpusID:272095987.

[68] Qiaoqiao Zhao and Feng He. “H- and J-aggregation of conjugated small molecules in organic solar cells”. In: *Journal of Energy Chemistry* (2024). URL: https://api.semanticscholar.org/CorpusID:267214585.

[69] Niko Van den Brande et al. “2. Phase Behavior in the Active Layer of Small Molecule Organic Photovoltaics: State Diagram of p-DTS(FBTTh2)2:PC71BM”. In: *Journal of Physical Chemistry C* (2020).

[70] Mitu Chauhan, Ram Sevak Singh, and Arun Kumar Singh. “1. Aggregation Induced Strong Photoluminescence at Room Temperature in Large-Area C8BTBT Thin Films”. In: *Synthetic Metals* (2024).

[71] Mitu Chauhan, Ram Sevak Singh, and Arun Kumar Singh. “Aggregation Induced Strong Photoluminescence at Room Temperature in Large-Area C8BTBT Thin Films”. In: *Synthetic Metals* (2024). URL: https://api.semanticscholar.org/CorpusID:269199241.

[72] Dipankar Gogoi and Tushar Dhabal Das. “2. Influence of highly optimized charge carrier mobility and diverse physical features toward efficient organic solar cells”. In: *Physica Scripta* (2024).

[73] Qiaoqiao Zhao and Feng He. “1. H- and J-aggregation of conjugated small molecules in organic solar cells”. In: *Journal of Energy Chemistry* (2023).

[74] Fabian Panzer et al. “2. A Unified Picture of Aggregate Formation in a Model Polymer Semiconductor during Solution Processing”. In: *Advanced Functional Materials* (2024).

[75] Qiaoqiao Zhao et al. “Balancing the H- and J-aggregation in DTS(PTTh2)2/PC70BM to yield a high photovoltaic efficiency”. In: *Journal of Materials Chemistry C* 3 (2015), pp. 8183–8192. URL: https://api.semanticscholar.org/CorpusID:93339705.

[76] Guo Chen et al. “J-aggregation of a squaraine dye and its application in organic photovoltaic cells”. In: *Journal of Materials Chemistry C* 1 (2013), pp. 6547–6552. URL: https://api.semanticscholar.org/CorpusID:95701999.

[77] Olivier J. Dautel et al. “Nanostructuration of phenylenevinylenediimide-bridged silsesquioxane: from electroluminescent molecular J-aggregates to photoresponsive polymeric H-aggregates.” In: *Journal of the American Chemical Society* 128 14 (2006), pp. 4892–901. URL: https://api.semanticscholar.org/CorpusID:43886538.

[78] Petter Paulsen Thoresen et al. “Role and importance of solvents for the fractionation of lignocellulosic biomass”. In: *Bioresource Technology* 369 (2023), p. 128447.

[79] Saunak Das and Martin Presselt. “Progress and development in structural and optoelectronic tunability of supramolecular nonbonded fullerene assemblies”. In: *Journal of Materials Chemistry C* 7.21 (2019), pp. 6194–6216.

[80] Heejoo Kim, Won-Wook So, and Sang-Jin Moon. “The importance of post-annealing process in the device performance of poly (3-hexylthiophene): Methanofullerene polymer solar cell”. In: *Solar Energy Materials and Solar Cells* 91.7 (2007), pp. 581–587.

[81] Kaichen Gu et al. “9. Role of Postdeposition Thermal Annealing on Intracrystallite and Intercrystallite Structuring and Charge Transport in Poly(3-hexylthiophene).” In: *ACS Applied Materials Interfaces* (2021).

[82] Shahin Maaref et al. “Molecular morphological effects to optoelectronics”. In: *SPIE Organic Photonics + Electronics*. 2007. URL: https://api.semanticscholar.org/CorpusID:94981421.

[83] Andrei V. Bogdanov and Vladimir F. Mironov. “4. Recent advances in the application of isoindigo derivatives in materials chemistry.” In: *Beilstein Journal of Organic Chemistry* (2021).

[84] V. Timofeev et al. “1. Effects of high-temperature annealing on vacancy complexes and luminescence properties in multilayer periodic structures with elastically strained GeSiSn layers”. In: (2024).

[85] Qiuju Liang et al. “7. Recent advances in effect of crystallization dynamics process on the morphology of active layer in organic solar cells”. In: *Battery energy* (2024).

[86] Vijay Kumar Baliyan et al. “Polarized photoluminescence of the polymer networks obtained by in situ photopolymerization of fluorescent monomer in a nematic liquid crystal”. In: *Optical Materials Express* 6.9 (2016), pp. 2956–2965.

[87] Michele Turelli et al. “Organic compounds for solid state luminescence enhancement/aggregation induced emission: a theoretical perspective”. In: *Physical Chemistry Chemical Physics* 25.27 (2023), pp. 17769–17786.

[88] Frank C. Spano. “The spectral signatures of Frenkel polarons in H- and J-aggregates.” In: *Accounts of chemical research* 43 3 (2010), pp. 429–39. URL: https://api.semanticscholar.org/CorpusID:33185753.

[89] Michael Kasha, H. Ralph Rawls, and M. Ashraf El-Bayoumi. “The exciton model in molecular spectroscopy”. In: *Pure and Applied Chemistry* 11 (1965), pp. 371–392. URL: https://api.semanticscholar.org/CorpusID:37647870.

[90] Nicholas J. Hestand and Frank C. Spano. “Molecular Aggregate Photophysics beyond the Kasha Model: Novel Design Principles for Organic Materials.” In: *Accounts of chemical research* 50 2 (2017), pp. 341–350. URL: https://api.semanticscholar.org/CorpusID:206381674.

[91] Ju Won Lim. “1. Polymer Materials for Optoelectronics and Energy Applications”. In: *Materials* (2024).

[92] Kamrun N. Keya et al. “2. Photoluminescence of Cis-Polyacetylene Semiconductor Material”. In: *Applied Sciences* (2022).

[93] Jeremy H. Burroughes et al. “Light-emitting diodes based on conjugated polymers”. In: *Nature* 347 (1990), pp. 539–541. URL: https://api.semanticscholar.org/CorpusID:43158308.

[94] An Gao et al. “Photoluminescence-based detection of particle contamination on extreme ultraviolet reticles.” In: *The Review of scientific instruments* 86 6 (2015), p. 063109. URL: https://api.semanticscholar.org/CorpusID:35807646.

[95] Zakir Çaldıran and Şakir Aydoğan. “Effects of the photoactive layer properties and current transmission mechanism on optical and electrical characteristics of organic photovoltaic”. In: *Optik* 241 (2021), p. 166937. URL: https://api.semanticscholar.org/CorpusID:235516338.

[96] Yan Meng et al. “Interchain coupling effects on dynamics of photoexcitations in conjugated polymers.” In: *The Journal of chemical physics* 128 18 (2008), p. 184903. URL: https://api.semanticscholar.org/CorpusID:18029443.

[97] Xin Chang, Mohammad Balooch Qarai, and Frank C. Spano. “HJ-aggregates of donor-acceptor-donor oligomers and polymers.” In: *The Journal of chemical physics* 155 3 (2021), p. 034905. URL: https://api.semanticscholar.org/CorpusID:236199543.

[98] Xiaoming Hu et al. “J-Aggregation Strategy toward Potentiated NIR-II Fluorescence Bioimaging of Molecular Fluorophores”. In: *Advanced Materials* 36 (2023). URL: https://api.semanticscholar.org/CorpusID:260376713.

[99] Theresa Eder et al. “Vibrations Responsible for Luminescence from HJ-Aggregates of Conjugated Polymers Identified by Cryogenic Spectroscopy of Single Nanoparticles.” In: *ACS nano* (2022). URL: https://api.semanticscholar.org/CorpusID:248049500.

[100] Chenyi Yang et al. “Molecular design of a non-fullerene acceptor enables a P3HT-based organic solar cell with 9.46% efficiency”. In: *Energy and Environmental Science* 13 (2020), pp. 2864–2869. URL: https://api.semanticscholar.org/CorpusID:224916033.

[101] Yilei Wu et al. “Fine-Tuning Semiconducting Polymer Self-Aggregation and Crystallinity Enables Optimal Morphology and High-Performance Printed All-Polymer Solar Cells.” In: *Journal of the American Chemical Society* (2019). URL: https://api.semanticscholar.org/CorpusID:208610856.

[102] Fei Dou et al. “Controlling Molecule Aggregation and Electronic Spatial Coherence in the H-Aggregate and J-Aggregate Regime at Room Temperature”. In: *Polymers* 12 (2020). URL: https://api.semanticscholar.org/CorpusID:215408277.

[103] Benjamin Hämisch and Klaus Huber. “Mechanism and equilibrium thermodynamics of H- and J-aggregate formation from pseudo isocyanine chloride in water.” In: *Soft matter* 17 35 (2021), pp. 8140–8152. URL: https://api.semanticscholar.org/CorpusID:237535685.

[104] *1. Modeling vibronic spectra of linear aggregates in MATLAB*. 2022. DOI: 10.26434/chemrxiv-2022-n28t1.

[105] Louis A. Perez et al. “The Role of Solvent Additive Processing in High Performance Small Molecule Solar Cells”. In: *Chemistry of Materials* 26 (2014), pp. 6531–6541. URL: https://api.semanticscholar.org/CorpusID:102154411.

[106] Ana M Gómez et al. “Naturally J-aggregated F-BODIPYs: Self-assembly organization driven by substitution pattern”. In: *Journal of Molecular Liquids* (2023). URL: https://api.semanticscholar.org/CorpusID:266155870.

[107] Kerstin S. Wienhold et al. “Effect of Solvent Additives on the Morphology and Device Performance of Printed Non-fullerene Acceptor Based Organic Solar Cells.” In: *ACS applied materials & interfaces* (2019). URL: https://api.semanticscholar.org/CorpusID:204866224.

Appendix A

Light Absorption and Photoluminescence (PL) Spectroscopy

Photoluminescence (PL) spectroscopy is a technique used to study the electronic properties of materials by analyzing the light they emit after being excited by light. When light, typically of a specific wavelength, is shone onto a sample, it excites the electrons within the material, causing them to transition from their ground state to a higher energy state. This process is known as photo-excitation. After a short period, the excited electrons return to their equilibrium state, releasing energy in the form of light, known as relaxation. The emitted light, or photoluminescence, carries valuable information about the material's electronic structure and behavior.

The photoluminescence spectrum can be interpreted through two key aspects: the absorbance spectrum and the emission spectrum. The absorbance spectrum is obtained by measuring how different wavelengths of light are absorbed to excite the electrons, with the emission being monitored at a fixed wavelength. This is represented by the blue line in Figure 2. The absorbance spectrum helps determine the appropriate excitation wavelength for subsequent measurements. The emission spectrum, shown as the red line in Figure 2, is then created by using a fixed excitation wavelength while varying the observed emission wavelengths. The intensity of the emitted light is plotted against wavelength to provide information about the peak emission intensity of the material. This peak is particularly useful for comparing the electronic properties of different materials, giving insight into the electronic structure and potential applications of the material in optoelectronics, semiconductors, and more.

In the figures provided, the excitation process (Figures 1a-c) shows how light energy elevates electrons to higher energy levels, which eventually relax back to their lower energy state, emitting light. The PL spectrum (Figure 2) then illustrates the specific wavelengths of light absorbed and emitted by the sample.

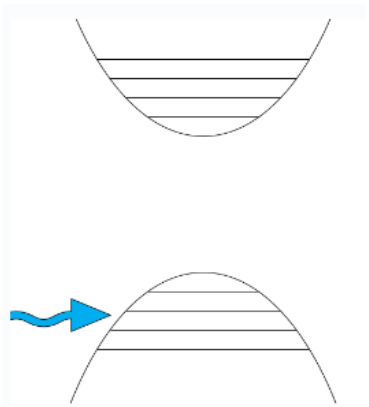

Figure 1: absorption of hf

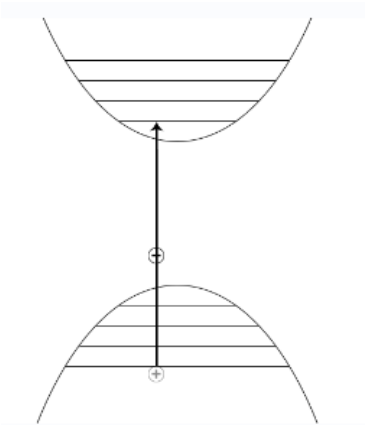

Figure 2: excitation of the e^{-s}

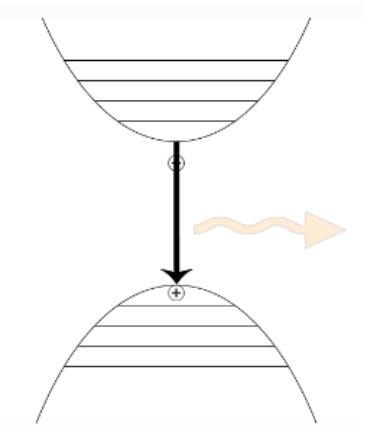

Figure 3: relaxation of the excited e^{-s}

Figure 4: These diagrams illustrate how light energy excites electrons to higher energy levels, which eventually relax back to their lower energy state, emitting light.